Archived version from NCDOCKS Institutional Repository http://libres.uncg.edu/ir/asu/

Appalachian
STATE UNIVERSITY
BOONE, NORTH CAROLINA

Southeastern Geology: Volume 47, No. 4 November 2010

Editor in Chief: S. Duncan Heron, Jr.

Abstract

Academic journal published quarterly by the Department of Geology, Duke University.

Heron, Jr., S. (2010). Southeastern Geology, Vol. 47 No. 4, November 2010. Permission to re-print granted by Duncan Heron via Steve Hageman, Professor of Geology, Dept. of Geological & Environmental Sciences, Appalachian State University.

SOUTHEASTERN GEOLOGY

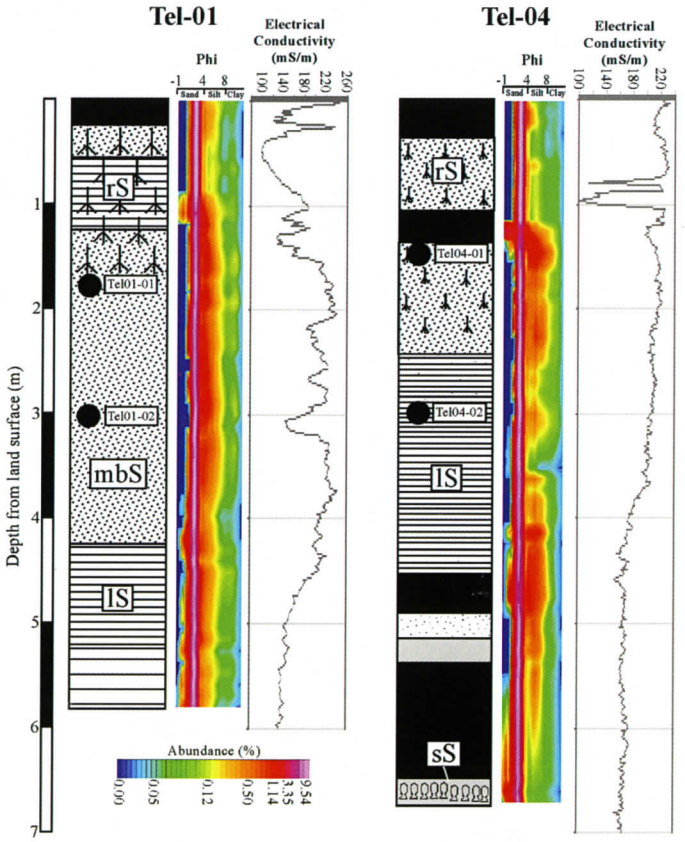

Vol. 47, No. 4 November 2010

SOUTHEASTERN GEOLOGY

PUBLISHED

at

DUKE UNIVERSITY

Duncan Heron

Editor-in-Chief

David M. Bush

Editor

This journal publishes the results of original research on all phases of geology, geophysics, geochemistry and environmental geology as related to the Southeast. Send manuscripts to **David Bush, Department of Geosciences, University of West Georgia, Carrollton, Georgia 30118, for Fed-X, etc. 1601 Maple St.,** Phone: 678-839-4057, Fax: 678-839-4071, Email: dbush@westga.edu. Please observe the following:

1) Type the manuscript with double space lines and submit in duplicate, or submit as an Acrobat file attached to an email.
2) Cite references and prepare bibliographic lists in accordance with the method found within the pages of this journal. Data citations examples can be found at http://www.geoinfo.org/TFGeosciData.htm
3) Submit line drawings and complex tables reduced to final publication size (no bigger than 8 x 5 3/8 inches).
4) Make certain that all photographs are sharp, clear, and of good contrast.
5) Stratigraphic terminology should abide by the North American Stratigraphic Code (American Association Petroleum Geologists Bulletin, v. 67, p. 841-875).
6) Email Acrobat (pdf) submissions are encouraged.

Subscriptions to *Southeastern Geology* for volume 47 are: individuals - $26.00 (paid by personal check); corporations and libraries - $40.00; foreign $55. Inquiries should be sent to: **SOUTHEASTERN GEOLOGY, DUKE UNIVERSITY, DIVISION OF EARTH & OCEAN SCIENCES, BOX 90233, DURHAM, NORTH CAROLINA 27708-0233**. Make checks payable to: *Southeastern Geology*.

Information about **SOUTHEASTERN GEOLOGY** is on the World Wide Web including a searchable author-title index 1958-2010 (Acrobat format). The URL for the Web site is: http://www.southeasterngeology.org

SOUTHEASTERN GEOLOGY is a peer review journal.

ISSN 0038-3678

SOUTHEASTERN GEOLOGY

Table of Contents

Volume 47, No. 4 September 2010

Serials Department
Appalachian State Univ. Library
Boone, NC

SOUTHEASTERN GEOLOGY
V. 47, No.4, November 2010, p. 175-190

GEOLOGIC INVESTIGATION AND OPTICAL DATING OF THE MERRITT ISLAND SAND RIDGE SEQUENCE, EASTERN FLORIDA, USA

BURDETTE, K.E.[A], RINK, W.J.[A], MALLINSON, D.J.[B], PARHAM, P.R.[B], REINHARDT, E.G.[A]

[a]*School of Geography and Earth Sciences, McMaster University, Hamilton, Ontario, Canada, L8S 4K1*

burdetke@mcmaster.ca

[b]*Department of Geological Sciences, East Carolina University, Greenville, NC, USA, 27858*

ABSTRACT

Ground penetrating radar (GPR) and the single-aliquot regenerative-dose (SAR) was used to determine the depositional environments and age of the Merritt Island sand ridge sequence. Five direct-push cores and ten OSL ages were collected. A new model of cosmic dose rate calculation, which removes the much younger aeolian cap, was utilized for the first time and helped produce more consistent OSL ages. Based on our data and samples, the Merritt Island sand ridges are a classic beach ridge set that was deposited during the MIS-5c sea-level highstand. This is supported by the results of Osmond (1970) based on U/Th ages and Burdette et al. (2009) based on OSL ages of a coquinoid limestone west of the beach ridge sequence.

INTRODUCTION

A multi-proxy approach was undertaken to determine the depositional history of a sand ridge sequence on Merritt Island, Florida. Ground penetrating radar (GPR) surveys allowed for the identification of radar facies that when coupled with defined lithofacies can be indicative of certain depositional environments (Burdette et al., 2009; Mallinson et al., 2010). Optically stimulated luminescence (OSL) dating allowed for burial age calculation of selected samples within the sequence and defined facies. Direct-push electrical conductivity (DPEC) allowed for high-resolution characterization of hydrostratigraphic features in the unconsolidated sediment.

Improved techniques in subsurface visualization utilizing GPR have led to an increase in its use in coastal environments (Van Heteren et al., 1994; Jol et al., 1996; Bristow et al., 2000; Jol et al., 2002; Mallinson et al., 2010). GPR can image high-resolution (cm scale) stratigraphy in shallow subsurface sand, gravel, and organic-rich material with the best results obtained in clean (free of silt and clay), quartz-rich, thick, clastic sediments (Smith and Jol, 1995). Van Heteren et al. (1994) developed one of the first tables that characterized various geometries and their relationship to the modern coastal facies. Bristow et al. (2000) conducted a similar GPR study of the foredunes in Norfolk, UK and identified seven different radar facies.

Luminescence dating methods encompass a range of techniques which, based on a radiation-produced charge population trapped within crystalline sedimentary materials, are capable of determining the period of time that has elapsed since the last time the trapped charge population was reset (Stokes, 1999). OSL fills an important niche in coastal geochronology where datable carbon or carbonates are absent or deposits of interest are beyond the range of radiocarbon dating. Numerous studies have been conducted on aeolian and coastal systems utilizing OSL with very encouraging results (Murray-Wallace et al., 2002; Berger et al., 2003; Tatumi et al., 2003, Frechen et al., 2004; Rink & Forrest, 2005; Lian and Roberts, 2006; Burdette, 2005; Mallinson et al., 2008a; Mallinson et al., 2008b; Wintle, 2008).

The measurement of the electrical resistivity (the inverse of conductivity) has long been used as a logging tool in open boreholes for both water well and oil well applications (Christy et al., 1994). The electrical conductivity associated with sedimentary materials varies with particle size, mineralogy, and matrix properties (Schulmeister et al., 2003). Silt- and sand-sized particles of covalently bonded minerals, such as

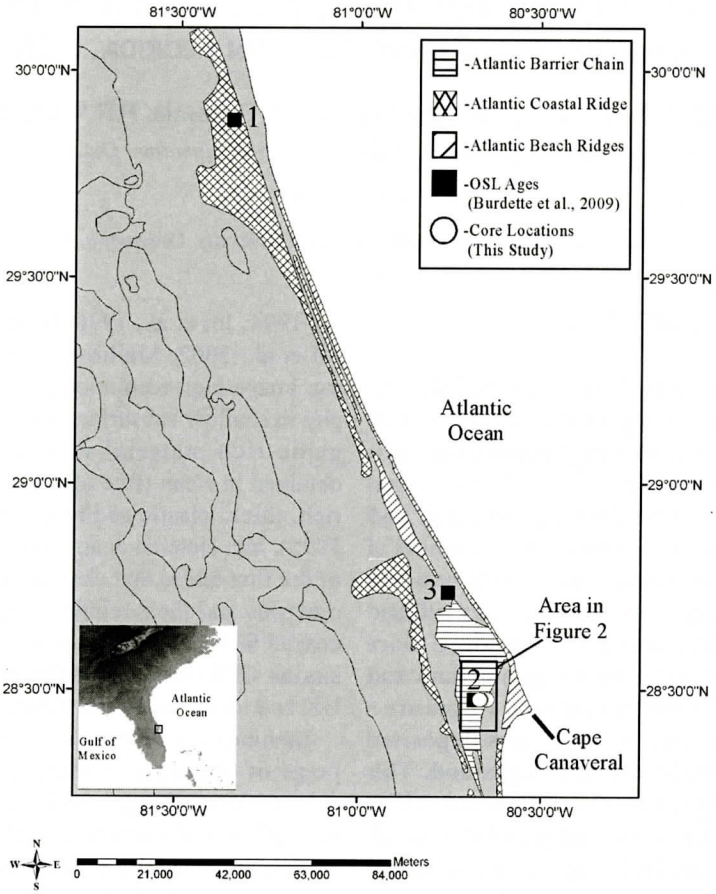

Figure 1. Physiographic map of eastern Florida showing the core locations from this study and sample locations from Burdette et al. (2009). Grey shaded areas are irrelevant physiographic nomenclatures. Location 1 – Wilson Coquina Quarry, Location 2 – Dalboro Road, Location 3 – Haulover Canal.

quartz, mica, and feldspar, are generally non-conductive, as opposed to clay-sized particles, which tend to be very conductive (Schulmeister et al., 2003). Therefore minute vertical changes in lithology and clay-sized particles can easily be detected and characterized using DPEC. In coastal sediments, the freshwater/saltwater interface may also be noted due to the contrast in resistivity.

By combining the use of these techniques, an accurate assessment of coastal evolution in response to process variables is possible. This manuscript presents data that reveal the accretion of a mixed carbonate-silisiclastic coastal system during multiple sea-level cycles of the late Pleistocene.

PREVIOUS REGIONAL WORK

The majority of the geologic work conducted in the Merritt Island/Cape Canaveral area predates or coincides with the development of the John F. Kennedy Space Center. Brown et al. (1962) conducted the first thorough geologic investigation of Brevard County and produced a table of the stratigraphic units of Brevard County, Florida (Table 1). Schmalzer and Hinkle (1990) used this table as well as core data from a preexisting National Aeronautics and Space Administration (NASA) report to generate two cross-sections on Merritt Island. The cross sections indicate that the upper ~40 ft (~12 m) is unconsolidated fine to medium sands of Pleisto-

Table 1. Stratigraphic units of Brevard County, Florida. Modified from Brown et al. (1962)

Geologic Age	Stratigraphic Unit		Approximate Thickness (m)	General Lithologic Character
Holocene	Pleistocene and Recent Deposits		0-33.5	Fine to medium sand, coquina and sandy shell marl
Pleistocene				
Pliocene	Upper Miocene and Pliocene deposits		6.1 – 27.4	Gray to greenish gray sandy shell marl, green clay, fine sand, and silty shell
Miocene	Hawthorn Formation		3.0 – 91.4	Light green to greenish gray sandy marl, streaks of greenish clay, phosphatic radiolarian clay, black and brown phosphorite, thin beds of phosphatic sandy limestone
Eocene	Ocala Group	Crystal River Formation	0 – 30.5	White to cream, friable, porous coquina in a soft, chalky marine limestone
		Williston Formation	3.0 – 15.2	Light cream, soft, granular marine limestone, generally finer grained than the Inglis Formation, highly fossiliferous
		Inglis Formation	21.3+	Cream to creamy white, coarse granular limestone, contains abundant echinoid fragments
	Avon Park Limestone		86.9+	White to cream, purple tinted, soft, dense chalky limestone. Localized zones altered to light brown or ashen gray, hard, porous, crystalline dolomite.

cene and Pliocene age.

Most of the arguments about the depositional age of Merritt Island are based on terrace location (Cooke, 1945; Kofoed and Gorsline, 1963; Alt and Brooks, 1965). Osmond et al. (1970) and later Rink and Forrest (2005) established absolute age controls on the formation of Merritt Island and Cape Canaveral. Brooks (1972) argued the western portion of Merritt Island to be Yarmouth glacial period (~240,000 yr ago) in age and the eastern sand ridge section to be Sangamon interglacial period (~132,000 - 71,000 yr ago) in age. The Yarmouth age is based on the discovery of the skeleton and teeth of *Archidiskodon haroldcooki*, a primitive mammoth that is distinctly found in the late Pleistocene Rancholabrean time (Brooks, 1972). The Sangamon age is based on the open-system U- series dating with modeling of shallow-water mollusk shells conducted by Osmond et al. (1970).

Osmond et al. (1970) performed U-Th age analysis on samples from nine locations around Brevard County, Florida. The nine samples clustered into three isochrons; modern, 30,000 yr ago, and 100,000 yr ago. The two samples collected in southeastern Merritt Island fall into the 30,000 yr ago and the 100,000 yr ago isochrons, even though they are only located a few miles apart. Kaufman et al. (1971) argued that dates obtained on mollusks by the U-series isotope methods are highly questionable and that isotope migration is a common phenomenon and occurs in ways which can neither be reliably corrected for, nor even detected. However, the ~30,000 yr ago age of Merritt Island was later roughly confirmed by Rink and Forrest (2005), who used OSL dates on sands derived from samples collected from the crest of a beach ridge (Figure 2).

Burdette et al. (2009) used OSL to date the deposition of the Anastasia Formation at three locations (Figure 1, locations 1, 2, and 3). Results confirm the finding of Osmond et al. (1970) and Mc-Neill (1985) that the upper coquinoid limestone of the Anastasia Formation dates to Marine Isotope Stage 5 (MIS-5) and the surficial deposits of this coquina were deposited

around 100 ka. Two of Burdette et al.'s (2009) OSL ages dated to MIS-5e (~112 ka) or MIS-5c (~105 ka): 1) at Wilson Coquina Quarry on the Atlantic Coastal Ridge west of St. Augustine and 2) on Merritt Island's Dalboro Road in the Atlantic Barrier Chain just west of our transect presented herein. The elevation of the Wilson Coquina sample suggests that relative sea level during one of these times reached approximately 8 m above present. The third location at Haulover Canal (location 3 on Figure 1) dates to MIS-5a (~83 ka) and suggests that relative sea level during MIS-5a reached to slightly above present sea level at that location in the Atlantic Barrier Chain. The results presented by Burdette et al. (2009) also confirm Brooks' (1972) idea that "the Anastasia was formed during several events..." based on three MIS-5 OSL ages. The first two OSL ages date to MIS-5e (~112 ka) or MIS-5c (~105 ka) and suggests that relative sea level during one of these times reached approximately 8 m above present. The third dates to MIS-5a (~83 ka) and suggests that sea level during MIS-5a reached approximately 2 m above present sea level.

Rink and Forrest (2005) also used OSL to place absolute age controls on the deposition of beach ridges on Cape Canaveral, Merritt Island, and mainland Brevard County. The majority of their study was conducted on Cape Canaveral with only one OSL age in Merritt Island. This sample was collected in the northeastern part of Merritt Island at a depth of ~100 cm below ground surface (Figure 2). The age of this sample (CC8) was 43,750 ± 3,640 yr ago.

METHODS

Geophysical

Four and a half kilometers of GPR data were collected throughout the study area in order to define radar facies and reflectors that are indicative of specific depositional environments (Figure 2). Data were collected along a single shore-normal (east-west) transect.

GPR data were acquired using a truck traveling between 3 and 5 miles per hour. A Geophysical Survey Systems Inc.© (GSSI) 200 MHz antenna was towed behind the truck while the passenger monitored the readout on the Subsurface Interface Radar (SIR) 2000 and collected notes. Data were collected at 16 bits/sample, 512 samples/scan, and 8 scans/second (approximately 6 scans/meter). Navigation data, recorded in WGS84 format, were obtained using a WAAS enabled Garmin 76CSx Global Positioning System (GPS) unit, which the driver monitored. Waypoints were recorded simultaneously on the GPR and GPS systems.

The raw GPR data were processed using Radan software©, which included bandpass filtering (75-225 MHz), gain adjustment, and stacking (3x). Processed data were exported as bitmap files into Canvas©. The major reflectors were traced and separated from the GPR line to help visualize depositional groups and define radar facies.

Two core locations (Tel-01 and Tel-04) were drilled using a direct-push EC logger (Figure 2). Data were collected every 0.015 m and depth was measured using a rig-mounted potentiometer. The data were stored in spreadsheet form, and then plotted on a graph of depth (m) vs. electrical conductivity (mS/m).

Sample Strategy & Acquisition

Five core locations were chosen using the GPR data in an attempt to recover multiple lithofacies in a single core (Figure 2). Core locations were documented using a Garmin 76CSx GPS unit. Four of the cores (Tel-01, Tel-02, Tel-03, & Tel-05) penetrated ~20 ft (~5.8 m) and Tel-04 penetrated ~24 ft (~7.0 m). After each core was collected and visually logged in the field, a second hole directly beside the original was drilled for optical dating samples. An opaque core liner was used and the desired depth was sampled. The core liners were then extracted directly into a 2.5 mm- thick black bag and taped closed.

Lithology

In the laboratory, the cores were opened, visually logged, photographed, and sampled for lithology. Laser diffraction particle size analy-

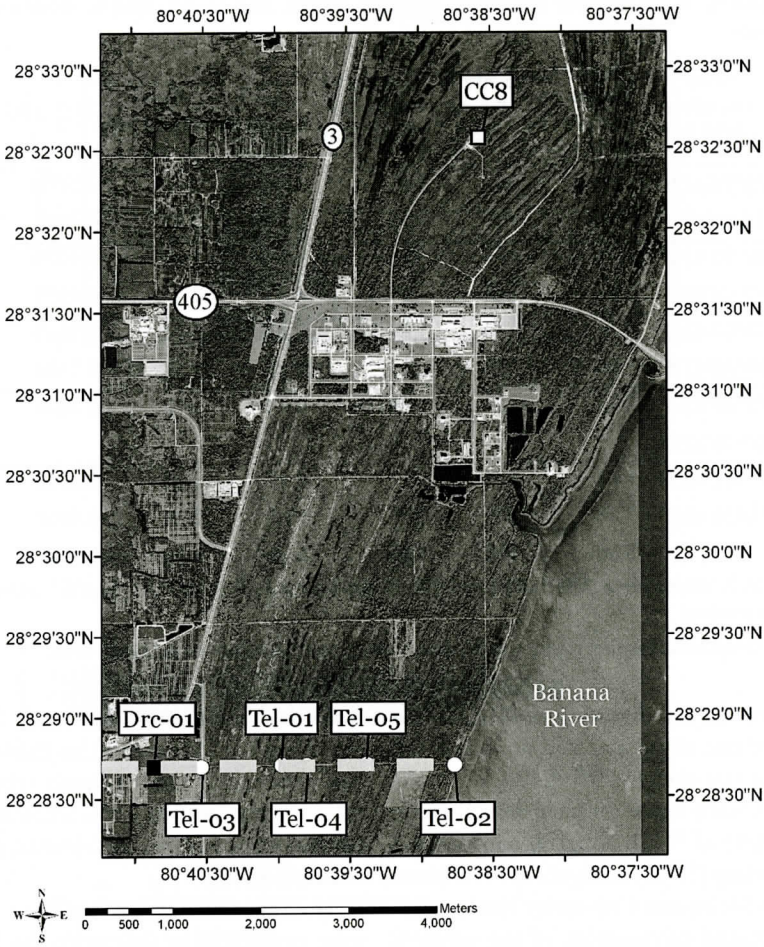

Figure 2. Digital Orthophoto Quarter Quad of eastern Merritt Island illustrating macrocore locations, coquina sample (Burdette et al., 2009), and OSL sample location (Forrest and Rink, 2005). Dashed grey line represents GPR transect.

sis was conducted on a Beckman-Coulter LS 230 (BC LS 230) at 10 cm intervals and mathematical computations were computed for each sample using the Fraunhofer optical model (Murray, 2002). Surface plots were constructed using Geosoft Oasis© for all cores as outlined by Beierle et al. (2002). Surface plots of grain size data allow qualitative interpretation of the characteristics of the entire particle size distribution (PSD) and thus can provide important insights into depositional processes and changing environmental conditions Beierle et al. (2002).

Optical Dating

All optically-dated samples were processed at the School of Geography and Earth Sciences at McMaster University under UV-filtered subdued orange light. Pure quartz grains were obtained using standard OSL preparation methods which include HCl and H_2O_2 digestions to remove carbonates and organics respectively, sieving to obtain desired grain size, heavy liquid separation using Lithium Polytungstate to remove heavy minerals and feldspars, HF digestion to remove the outer alpha effected layer, a second H_2O_2 digestion to remove any remaining feldspars and any fluorides that may have

Table 2. Location, approximate elevation, sample depth, and U, Th, and K values of the Merritt Island samples

Sample Name	Core Location (WGS 84)	Approx Elevation relative to MSL (m)	Sample Depth (cm)	Corrected Sample Depth (cm)	U^{238} (ppm) [a]	Th^{232} (ppm) [a]	K (%) [a]	Water Content (%) [b]
Tel03-03	28°28'41.6"	0.44	56	N/A	0.24	0.30	0.0055	2.72
Tel03-01	80°40'32.1"	-3.12	456	356	0.68	0.29	0.0205	7 (14.15)
Tel01-01	28°28'42.2"	-0.77	177	77	0.35	1.40	0.1076	7 (19.28)
Tel01-02	80°39'58.7"	-2.81	304	204	0.21	0.33	0.1933	7 (25.82)
Tel04-01	28°28'42.2"	-0.28	128	28	0.59	0.83	0.1645	7 (29.27)
Tel04-02	80°39'47.5"	-1.98	298	198	0.42	0.56	0.1927	7 (29.26)
Tel05-01	28°28'42.4" 80°39'22.9"	-2.98	298	198	0.74	0.62	0.3804	7 (26.83)
Tel02-03	28°28'42.1"	-1.77	177	77	0.76	2.25	0.0653	7 (24.36)
Tel02-01	80°38'46.0"	-3.36	336	236	0.40	0.71	0.5360	7 (28.18)
Tel02-02		-5.36	536	436	0.85	0.89	0.7026	7 (32.14)

[a] U, Th, and K values were determined by NAA on sub-samples derived from the OSL samples prior to chemical treatments.

[b] Water content as a fraction of dry weight determined from laboratory measurements.

formed during the HF digestion, and finally re-sieving to remove any grains that no longer fall in the desired size range (150 – 212 μ).

Dose rates were based on neutron activation analysis (NAA) of ^{232}Th and ^{40}K and delayed neutron counting (DNC) analysis of ^{238}U (conducted at the McMaster University Nuclear Reactor). Untreated subsamples of the original samples were used to determine the elemental concentrations of radioactive ^{238}U, ^{232}Th and ^{40}K (Table 2). NAA/DNC-based dose rates were calculated assuming radioactive equilibrium in the ^{238}U and ^{232}Th decay chains.

Luminescence measurements were conducted on a RISØ OSL/TL-DA-15 reader using blue light LED stimulation (470 nm) and a 7 mm-thick Hoya U-340 filter (270–400 nm). A calibrated ^{90}Sr beta source was used to perform laboratory irradiations. The single aliquot regeneration (SAR) protocol (Murray and Wintle, 2000) was conducted on a minimum of 24 aliquots to determine a final equivalent dose (De). Quartz grains, between 150-212 microns, were mounted with silicon spray on aluminum discs using a 3mm and a 1mm mask and were illuminated for 100 seconds at 125° C. The background (the last 4 s) of the OSL decay curve was subtracted from the "fast" component (first 0.4 s) to determine the samples luminescence signal. Only aliquots whose recycling ratios were within 10% were accepted for equivalent dose (De), also known as paleodose, determination.

Thermal transfer test and dose recovery test were performed to determine the final De preheat temperature (Madsen et al., 2005). For both tests, twelve aliquots from each sample were optically bleached by blue light illumination for 40 seconds, followed by a 10,000 second pause and another 40-second illumination. For the dose recovery test, the aliquots were given a known dose. Both tests continued with the standard SAR protocol except the preheat temperatures varied (160, 200, 240, 280° C), with 3 aliquots from each sample receiving a different preheat temperature. For each sample the dose recovery test was used to determine which preheat temperature produced a De closest to the given dose. Once this preheat temperature was determined the thermal transfer test was analyzed to ensure there was no induced charge transfer at that given temperature.

A feldspar contamination check, as outlined by Thompson et al. (2007), was also performed

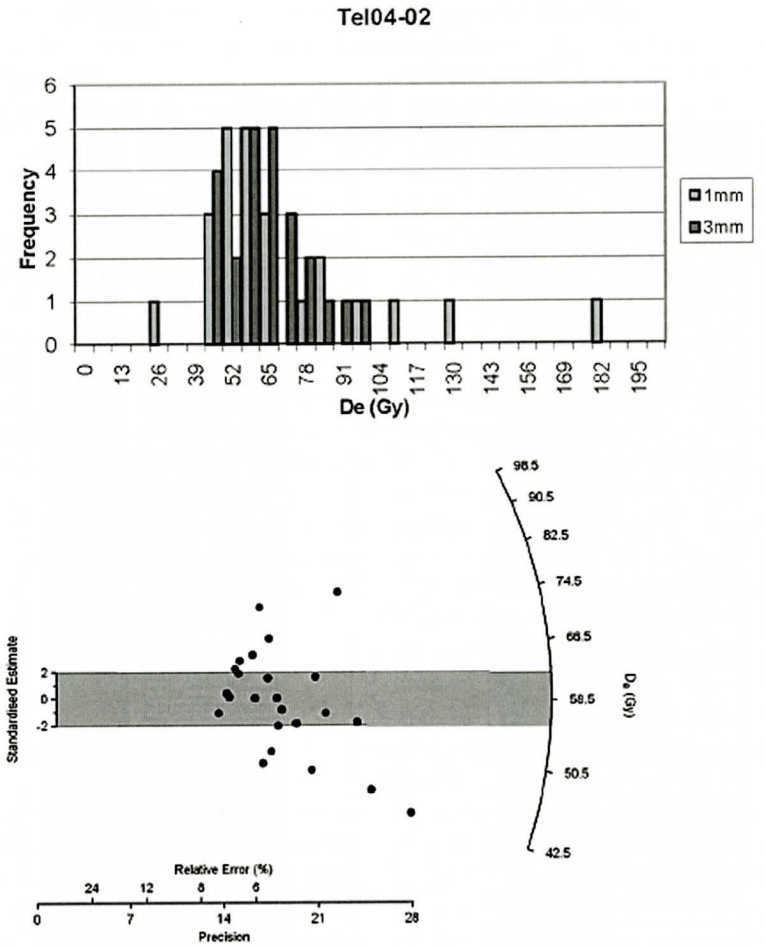

Figure 3. Histogram and Radial Plot of Tel04-02.

on each sample to ensure purity of the quartz grain separates. An initial De was estimated by comparing the natural OSL signal (preheat T = 200°C) of 3 aliquots to the regenerated OSL given by a single dose. A second identical regeneration dose was applied to the same aliquots and the IRSL signal was measured. If a ratio of IRSL to regenerated OSL signal was less than 1% for all aliquots, it is assumed there is no significant feldspar contamination (Forrest et al., 2003).

Moisture contents were measured in the lab from the recovered sediment and used for the dose rate calculations for the younger samples. If the samples were deposited before the last glacial maximum (LGM), then a moisture of 7% was used as an estimate of the moisture content throughout the samples burial history. The internal ^{238}U and ^{232}Th dose rates were calculated using the average concentration of those radioisotopes in granitic quartz (Rink and Odom, 1991), using an alpha efficiency factor of 0.04 +/- 10%. Cosmic ray dose rates were calculated using the burial depth and a 2 g/cm^3 of overburden density using calculations by Prescott and Hutton (1988) with the ANATOL program version 0.72B (provided by N. Mercier, CNRS, Paris). Burial depth was determined by using the linear accumulation model or instant accumulation model. The linear accumulation model assumes sedimentation has been constant throughout its depositional history and not instantaneous. For the linear accumulation model, one half the true burial depth is used in

Figure 4. Core sedimentology log, PSD, and electrical conductivity of Tel-01 and Tel-04. Black areas represent no core recovery. Black circles represent OSL sample locations. Rooted Sand=rS, Massively Bedded Sand= mbS, Laminated Sand=lS, Shelly Sand=sS.

the cosmic dose calculation.

De values and their associated errors for each aliquot were calculated using an exponential plus linear function in the RISØ Luminescence Analyst program (version 3.15b). Over-dispersion and De for each sample were calculated using the Central Age Model (written by S. Huot and provided by R. Roberts). The Central Age Model explicitly determines the extent of De over-dispersion between aliquots, and takes this into account when estimating the mean De values and their precisions (Galbraith et al., 2005). Over-dispersion is defined as the relative standard deviation of the De estimates, above and

beyond that due to photon counting statistics and curve-fitting uncertainties (Roberts and Galbraith, in press).

Histograms, comparing the 3mm mask data and the 1mm mask data, and radial plots were constructed to graphically display the De distributions (Figure 3). Histograms are effective at illustrating the shape of a distribution (in addition to its location and spread), however they do not take into account the precision associated with each De value (Roberts and Galbraith, in press). Therefore, in addition to histograms, radial plots were constructed. A radial plot is a graphical display for comparing estimates that have differing precision (Galbraith, 2005). It is essentially a scatter plot that plots a standardized estimate on the y-axis against the precision (defined as the reciprocal of the standard error of the estimate) on the x-axis (Roberts and Galbraith, in press).

RESULTS

Geophysics

Ground penetrating radar and lithologic descriptions were used to define radar facies (RF). RF1 is characterized by continuous, high amplitude, horizontal reflectors and is uniformly one to two meters in thickness. RF1 is identified as remobilized sands or an aeolian sand sheet (Figure 6). RF2 is characterized by continuous (>10m), low-angle landward dipping (westward-dipping) clinoforms and is interpreted as an overwash fan or and aeolian sand sheet. RF2 appears to begin around Tel-03 and end around Tel-04. RF3 is characterized by discontinuous, low to medium amplitude, seaward dipping (eastward-dipping) clinoforms and is interpreted as beach ridge foreslope accretion. RF3 has been identified by numerous authors in marine and lacustrine environments (Van Heteren, 1994; Jol et al., 1996; Bristow et al., 2000; Burdette, 2005; Mallinson et al., 2008a; Burdette and Mallinson, 2008).

Lithology

Figures 4 and 5 illustrate the homogeneity of the sediments that compose the upper ~6m of the Merritt Island sand ridge sequence. The PSD plots for Tel-01 and Tel-04 demonstrate clearly that although the mean grain size remains nearly constant downcore, variations in silt concentrations are partly responsible for differentiating lithofacies. Without the use of the PSD plots these variations may have gone unnoticed. The fluctuations in the EC mimic the PSD color variations and appear to be controlled largely by the abundance of clays. Conductivity is generally highest where clay content is high. It should be noted that EC graphs are a relative graph and can not independently determine grain size. Therefore EC graphs should always be ground-truthed with a separate method such as grain-size analysis or in this case PSD.

Four lithofacies were defined in the Merritt Island sequence. Rooted sands (rS) occurred in the upper 2m of each core and represent the modern topsoil. These rooted sands correlate with RF1. The EC record that corresponds to rS is highly variable, which is expected with the roots and clay variations that make up the modern soils. Massively bedded sands (mbS) occur in most cores; however Tel-04 contained a ~3m section. The EC record that corresponds to the mbS in Tel-01, suggests varying amounts of silts and clays, shown in the irregularity of the record (Figure 4). Based on modern environments, massively bedded sands could represent several depositional environments including flood-tidal deltas, overwash fans, back-barrier sand flats, and aeolian deposits (Susman and Heron, 1979; Reinson, 1992; Culver et al., 2005).

Laminated sand (lS) was recognized in all the cores, except Tel-03, usually in the lower portion of the core. The EC record that corresponds with the lS in Tel-01 and Tel-04 is quite different than the mbS. The EC record of the lS in Tel-04 is a relatively smooth record with a gradual decrease in signal with depth. Typically, in coastal environments, heavy minerals cause the laminations, but this area lacks significant heavy mineral sands, therefore the laminations are created by slightly muddier sands or sands of a very minute grain size difference.

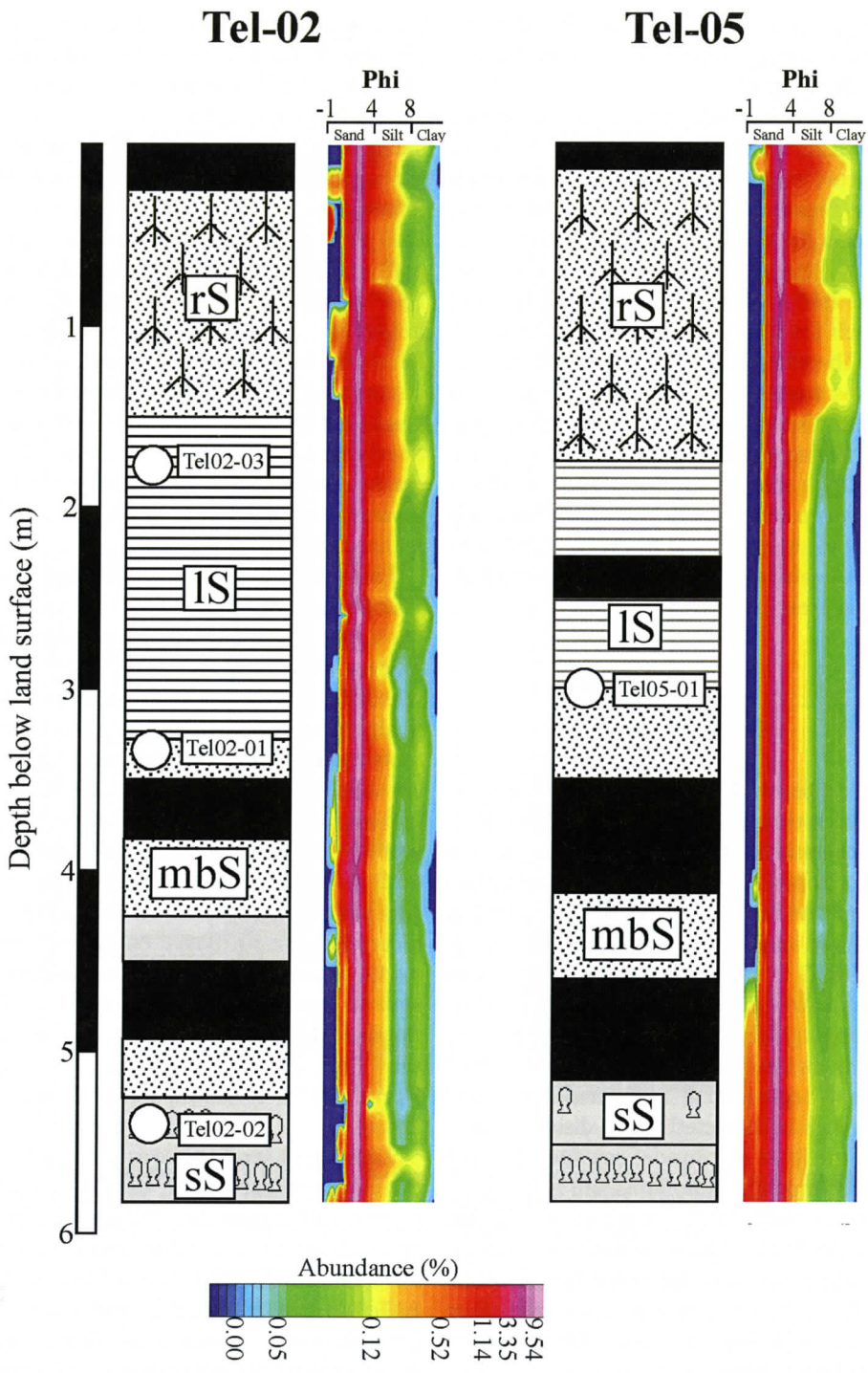

Figure 5. Core sedimentology log and PSD of Tel-02 and Tel-05. Black areas represent no core recovery. White circles represent OSL sample locations. Rooted Sand=rS, Massively Bedded Sand= mbS, Laminated Sand=lS, Shelly Sand=sS.

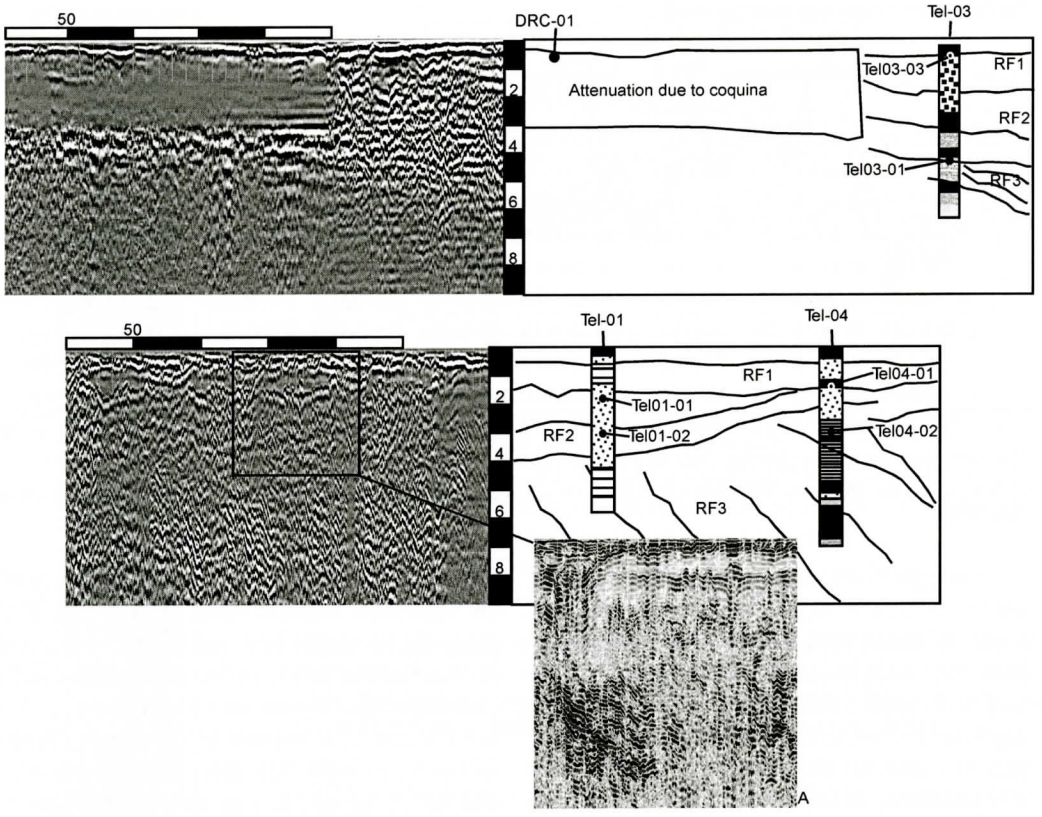

Figure 6. Ground penetrating radar sections (left) and interpretations with macrocore logs (right). Scale is in meters. Black area in core logs represent areas of no core recovery. Enlarged area A represents unstacked data to help visualize radar facies.

Laminated sands are typical of modern barrier island deposits in a variety of environments including flood-tidal deltas, distal overwash fans, foreshore and backshore deposits, aeolian dunes, and back-barrier berms (Susman and Heron, 1979; Culver et al., 2005).

Shelly sand (sS) was present in Tel-03 and at the base of Tel-04, Tel-02, and Tel-05. The shell and shell fragments were identified as *Donax sp.*, which live in the high energy swash zones of Florida's modern beaches. The shelly sand in Tel-03 was quite different from that in the other cores. It graded from a nearly cemented, very limey, shelly sand with shell concentrations around 25% (~2.8m-3.5m) to a nearly 50% highly fragmented shelly sand (~3.75m) that slowly graded into a shelly sand with only 2-5% shell fragments at the bottom of the core. It should be noted that Tel-03 was collected less than 100 yards from the edge of the coquina described in Burdette (2009) (Figure 6).

Optical Dating

The OSL ages cluster four groups. (Table 3) Group Four is includes Tel04-02 (113.6-133.6 ka) and is interpreted as being deposited during MIS-5e. Group Three includes Tel01-01 (89.2-103.4 ka), Tel01-02 (92.3-106.9 ka), Tel02-01 (92.2-110.8 ka), Tel02-03 (81.1-95.9 ka), Tel04-01 (83.1-94.1 ka), and Tel05-01 (77.3-91.1 ka) and is interpreted as being deposited during MIS-5c. Group Two includes Tel02-02 (70.7-84.3 ka), Tel03-01 (69.2-83.6 ka). Group Two is interpreted as being deposited during MIS-5a. Group One includes Tel03-03 (18.9-22.7 ka) and is interpreted as being deposited during the last glacial maximum.

Table 3. Luminescence dating results

Group	Sample Name	De (Gy)	s	Associated Radar Facies / Lithofacies	Cosmic Dose Rate (μGy/a) [c]	Beta Dose Rate (μGy/a) [c]	NAA/DNC Gamma Dose (μGy/a) [d]	Total External Dose (μGy/a)	Total Internal Dose (μGy/a)	SAR-OSL Age (KA)
1	Tel03-03	5.6±0.3	23	RF1 / rS	196.18±19.6	33.9±12.2	29.0±11.0	259.1±16.4	10.5±2.3	18.9 – 22.7
2	Tel02-02	79.0±4.0	25	N/A/ sS	118.47±11.9	599.3±17.9	290.5±11.9	1008.4±21.5	10.5±2.3	70.7 – 84.3
	Tel03-01	25.3±1.6	31	RF2 / sS	130.85±13.1	93.9±11.2	84.7±10.1	320.8±15.1	10.5±2.3	69.2 – 83.6
3	Tel01-01	45.0±2.0	23	RF2 / mbS	188.76±18.9	143.6±12.2	124.3±11.5	456.7±16.8	10.5±2.3	89.2 – 103.4
	Tel01-02	41.3±1.3	15	RF2 / mbS	159.14±15.9	163.8±12.7	81.2±10.9	404.2±16.8	10.5±2.3	92.3 – 106.9
	Tel02-01	80.0±5.0	29	N/A / lS	152.60±15.3	428.6±15.7	196.6±11.4	777.9±19.4	10.5±2.3	92.2 – 110.8
	Tel02-03	51.0±3.0	26	N/A / lS	188.76±18.9	180.4±12.4	196.3±12.5	565.4±17.6	10.5±2.3	81.1 – 95.9
	Tel04-01	50.4±1.3	11	RF2 / rS	221.87±22.2	199.1±12.7	137.3±11.6	558.3±17.2	10.5±2.3	83.1 – 94.1
	Tel05-01	61.0±3.0	26	N/A / lS	160.41±16.0	360.2±14.3	193.2±11.2	713.9±18.2	10.5±2.3	77.3 – 91.1
4	Tel04-02	59.0±3.0	20	RF3 / lS	160.41±16.0	192.8±12.4	113.6±10.9	466.9±16.6	10.5±2.3	113.6 – 133.6

[c] Cosmic dose rate value calculated using an overburden density of 2 g/cm^3.

[d] All β and γ dose rates were calculated based on U, Th, and K concentrations of each sample accounting for moisture values of the sample.

As is typical of Florida coastal environments, the low content of U, Th, and K render the total dose rate's composition to one with a large proportion of cosmic dose rate. We found it necessary to consider carefully the average burial depth for the entire history of burial in order to properly calculate the cosmic dose rate in these circumstances. In our sites there was an aeolian layer (RF1) that was conservatively estimated to be about 1m thick in all cores. This layer was probably deposited in the last 15,000 years or so, based on similar studies in the southeastern US (Ivester et al., 2001, Burdette, 2005, Mallinson et al, 2008a, Mallinson et al, 2008b). Therefore over the entire history of burial it was only present for a relatively short time and we had to adjust the depth of burial by employing a model that incorporated stripping off the overburden. We refer to this procedure used for the first time here the aeolian cap removal model (ACRM). Corrected sample depths are listed in Table 2. Until this model was used, the ages were less well clustered, mainly fell outside of MIS-5c, and were inconsistent with the geology.

DISCUSSION

The base of the Merritt Island sand ridge sequence is composed of seaward dipping clinoforms labeled in the radargrams as RF3 and identified as a foreshore deposit (Figure 6 and Figure 7). This interpretation is consistent with the lithofacies found in cores. In the cores, RF3 generally coincides with the lS lithofacies and in some cores (Tel02, Tel04, and Tel05) this lS lithofacies grades into an sS with depth (~5-6 m). The one OSL age that can clearly be identified as RF3 (Tel04-02), dates between 113.6 ka and 133.6 ka and has an over-dispersion of 20%. Also the histograms show no evidence of mixing or incomplete zeroing based on the decrease of mask size from 3mm to 1mm.

Tel02 and Tel05 were located at the eastern end of the transect (Figure 2) and due to the low elevation (0-1 m above mean sea level) and intrusion of brackish water, the radar signal was slightly attenuated. Tel02-01, Tel02-03, and Tel05-01 all cluster in MIS-5c, while Tel02-02 appears to have an anomalously young age associated with MIS-5a. The over-dispersions of the four samples are 29%, 26%, 26%, and 25%, respectively.

Radar facies RF2 is composed of low-angle landward dipping clinoforms and may represent back-barrier sand flats, consisting of overwash or aeolian sand sheet facies (Figure 6 and Figure 7). Four OSL samples were collected in RF2 (Tel01-01, Tel01-02, Tel03-01 and Tel04-01) with over-dispersions of 23%, 15%, 31%, and 11%, respectively. Three samples (Tel01-01, Tel01-02, and Tel04-01) cluster within MIS-5c (105 – 95 Ka), while Tel03-01 dates to

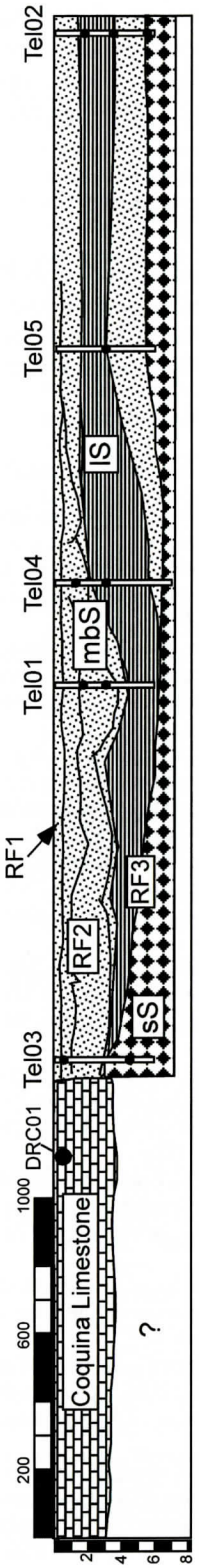

Figure 7. Cross section of the Merritt Island transect. Scale is in meters.

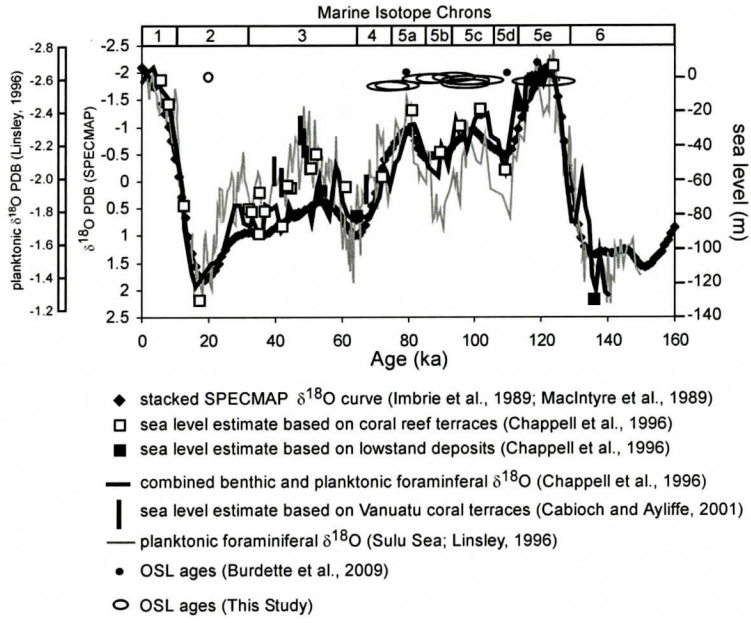

Figure 8. Comparison of the SPECMAP marine δ18O curve (Imbrie et al., 1989; MacIntyre et al., 1989), coral reef terraces (Chappell et al., 1996; Cabioch and Ayliffe, 2001), foraminiferal δ18O data (Chappell et al., 1996; Linsley, 1996), and OSL data (Burdette et al., 2009).

69.2 ka to 83.6 ka.

MIS-5c had a sea-level high stand that has been interpreted not to be as high globally as during MIS-5e and MIS-5a (Imbrie et al., 1989; MacIntyre et al., 1989; Chappell et al., 1996; Linsley, 1996; Cabioch and Ayliffe, 2001) (Figure 8). However some evidence suggests that regionally MIS-5c relative sea level did reach as high as MIS-5e and MIS-5a (Potter et al., 2004; Potter and Lambeck, 2004; Dumas et al., 2006; Coyne et al., 2007; Dutton et al., 2009; Parham, 2009). Therefore RF3 and RF2 are defined as a beach ridge and overwash sequence that was deposited during the MIS-5c highstand. The apparently anomalously younger MIS-5a ages for Tel03-01 and Tel02-02 both occur in the shelly sand unit. This suggests the possibility that there is a systematic problem with dating shelly sand with OSL (see also Burdette et al. 2009 for a discussion of the potential problems in dating coquina rock). The apparently anomalously old MIS-5e age for Tel04-02 comes from the laminated sand unit, and may be a result of upward mixing of older grains by bioturbation. However, the evidence of incomplete zeroing or mixing is not strongly supported by the overdispersion value of 20%, nor the histogram in Figure 3, though a few older aliquots were found at higher doses in the 1mm mask size than in the 3mm mask size.

Sea levels during cooler time periods (MIS 4 – MIS 2) were lower and sand became remobilized as an aeolian sand sheet, identified in the Merritt Island

sand sequence as RF1. Similar types of this uppermost sand unit have been recognized over most of the southeastern United States from Florida to Delaware in late Pleistocene deposits (Ivester et al., 2001; Mallinson et al., 2008a; Mallinson et al., 2008b). Mallinson et al (2008a) describes one of these units in eastern North Carolina as an uppermost, remobilized aeolian sand averaging 2 meters in thickness. Tel03-03 and probably CC8 (Rink and Forrest. 2005) were collected in this unit and support previous studies suggesting that this unit was deposited during late Quaternary cooler climates (Burdette, 2005; Mallinson et al., 2008a).

CONCLUSIONS

Our evidence suggests that RF3 and RF2 are components of a classic beach ridge deposit formed on the central eastern portion of Merritt Island at or near sea level during MIS-5c. Our OSL ages are in good agreement with the work of Osmond (1970), the hypothesis of Brooks (1972), and the work of Burdette et al. (2009). Although globally MIS-5c may not have reached the heights of MIS-5a or MIS-5e, in the southeastern United States there is mounting evidence that sea levels during MIS-5c did surpass present day sea level. The detailed lithologies and radar facies presented here form the first high-resolution transect for the Pleistocene of Merritt Island.

Capping the whole Merritt Island section is RF1, an aeolian sand sheet deposited as climate began to cool, sea level dropped, exposed sand became mobilized, and a sand sheet formed atop older deposits. This aeolian cap is recorded along the Atlantic coastal plain from Delaware to Florida. We found that use of the ACRM, described for the first time in this study, was essential for obtaining reliable OSL ages for environments with high proportions of cosmic dose rate.

Through this work and that of Burdette et al. (2009) we have shown that there is evidence for shoreline complexes at or near modern sea levels in both MIS-5a and 5c. However, there is the possibility that the Atlantic Coastal Ridge, at elevations up to 8m (as at Wilson Coquina Quarry), are the only preserved remnants of MIS- 5e along the coast, and that the lower shoreline complexes were deposited after significant erosion of the previously deposited MIS-5e complexes.

ACKNOWLEDGEMENTS

We are grateful for financial support to WJR from the Natural Sciences and Engineering Research Council of Canada (NSERC). We thank Chantel Iacoviello and Gloria Lopez for their assistance in the field.

REFERENCES CITED

Alt, D., Brooks, H.K., 1965. Age of the Florida Marine Terraces. Journal of Geology 73, 406-411.

Beierle BD, Lamoureux SF, Cockburn JMH, Spooner I, 2002. A new method for visualizing sediment particle size distribution. J Paleolimnol 27:279–283.

Berger et al., Murray, A.S., Havholm, K.G., 2003. Photonic dating of Holocene back-barrier coastal dunes, northern North Carolina, USA. Quaternary Science Review 22,1043-1050.

Bristow, C.S., Chroston, P.N., Bailey, S.D., 2000. The structure and development of foredunes on a locally prograding coast: insights from ground-penetrating radar surveys, Norfolk, UK. Sedimentology 47, 923-944.

Brooks, H.K., 1972. Geology of Cape Canaveral. Space Age Geology, Southeastern Geology Society, 16th Field Conference. Tallahassee, Florida: Southeastern Geological Society, 35–44.

Brown, D.W., Kenner, W.E., Crooks, J.W., Foster, J.B., 1962. Water Resources of Brevard County, Florida. Florida Geological Survey Report of Investigations No. 28, 157 p.

Burdette, K., 2005. Chronostratigraphy and geologic framework of the Currituck Sand Ridges, Currituck County, NC. Unpub. M.S. Thesis, Dept. of Geology, East Carolina University, Greenville, NC. 184 p.

Burdette, K., Rink, W.J., Means, G.H., Portell, R.W, 2009. Optical Dating of the Anastasia Formation, Northeastern Florida, USA. Southeastern Geology 46 (4), 173-185.

Burdette, K., Mallinson, D, 2008. Geologic Framework of the Currituck Sand Ridges, Northeastern North Carolina. Southeastern Geology 45 (1), 1-15.

Cabioch, G., Ayliffe, L.K., 2001. Raised coral terraces at Malakula, Vanuatu, Southwest Pacific, indicate high sea level during marine isotope stage 3. Quaternary Research 56, 357–365.

Chappell, J., Omura, A., Esat, A., McColluch, T., Pandolfi, M., Pillans, J., 1996. Reconciliation of Late Quaternary sea levels derived from coral terraces at Huon Peninsula with deep sea oxygen isotope records. Earth and Plan-

etary Science Letters 141, 227–236.

Cooke, C.W., 1945. Geology of Florida. Florida Geological Survey Bulletin 29, 342 p.

Coyne, M., Jones, B., Ford., D., 2007. Highstands during Marine Isotope Stage 5:evidence from the Ironshore Formation of Grand Cayman, British West Indies. Quaternary Science Reviews 26, 536-559.

Christy, C.D., 1994. A Percussion Probing Tool for the Direct Sensing of Soil Conductivity. Geoprobe Technical Paper No. 94-100, 16 p.

Culver, S.J., Ames, D.V., Corbett, D.R., Mallinson, D.J., Riggs, S.R., Smith, C.S., Vance, D.J., 2005. Foraminiferal and Sedimentary Record of Late Holocene Barrier Island Evolution, Pea Island, North Carolina: The Role of Storm Overwash, Inlet Processes, and Anthropogenic Modification. Journal of Coastal Research 21, 406-416.

Dumas, B., Hoang, C., Raffy, J., 2006. Record of MIS 5 sea-level highstands based on U/Th dated coral terraces of Haiti. Quaternary International 145-146, 106-118.

Dutton, A., Bard, E., Antonioli, F., Esat, T., Lambeck, K., McCulloch, M., 2009. Phasing and amplitude of sea-level and climate change during the penultimate interglacial. Nature Geoscience 470, 1-5.

Forrest, B.M., 2003. Application of luminescence techniques to coastal studies at the St. Joseph Peninsula, Gulf County, Florida. Unpub. M.Sc. Thesis, McMaster University, Hamilton, Canada.171 p.

Frechen, M., Neber, A., Tsatskin, A., Boenigk, W., Ronen, A., 2004. Chronology of Pleistocene sedimentary cycles in the Carmel Coastal Plain of Israel. Quaternary International 121, 41-52.

Galbraith, R.F., Roberts, R.G., Yoshida, H., Error variation in OSL paleodose estimates from single aliquots of quartz: a factorial experiment. Radiation Measurements 39, 289-307.

Imbrie, J., McIntyre, A., Mix, A.C., 1989. Oceanic response to orbital forcing in the late Quaternary: observational and experimental strategies. In: Berger, A., Schneider, S.H., Duplessy, J.C. (Eds.), Climate and Geosciences, a Challenge for Science and Society in the 21st Century. D. Reidel Publishing Company.

Ivester, A.H., Leigh, D.S., Godfrey-Smith, D.I., 2001. Chronology of Inland Eolian Dunes on the Coastal Plain of Georgia, USA. Quaternary Research 55, 293-202.

Jol, H.M., Smith, D.G., Meyers, R.A., 1996. Digital Ground Penetrating Radar (GPR): A new geophysical tool for coastal barrier research (examples from the Atlantic, Gulf, and Pacific Coasts, U.S.A.). Journal of Coastal Research 12(4), 960- 968.

Jol, H.M., Lawton, D.C., Smith, D.G., 2002. Ground Penetrating Radar:2-D and 3-D subsurface imaging of a coastal barrier spit, Long Beach, WA, USA.Geomorphology 53, 165-181.

Kaufman, A., Broecker, W.S., Ku, T.L., Thurber, D.L., 1971. The status of U-series methods of mollusk dating. Geochimica et Cosmochimica Acta 35, 1155-1183.

Koefoed, J., 1963. Coastal Development in Volusia and Brevard Counties, Florida. Bulletin of Marine Science of the Gulf and Caribbean 13, 1-10.

Lian, O.B., Roberts, R.G., 2006. Dating the Quaternary: Progress in Luminescence Dating of Sediment. Quaternary Science Reviews 25, 2449-2468.

Linsley, B., 1996. Oxygen-isotope record of sea level and climate variations in the Sulu Sea over the past 150,000 years. Nature 380, 234–237.

MacIntyre, A., Ruddiman, W.F., Karlin, K., Mix, A.C., 1989. Surface water response of the equatorial Atlantic Ocean to orbital forcing. Paleoceanography 4, 19–55.

Madsen, A.T., Murray, A.S., Anderson, T.J., Pejrup, M., Breuning-Madsen, H., 2005. Optically stimulated luminescence dating of young estuarine sediments: a comparison with 210Pb and 137Cs dating. Marine Geology 214, 251–268.

Mallinson, D., Burdette, K., Mahan, S., Brook, G., 2008a. Optically Stimulated Luminescence age controls on late Pleistocene and Holocene coastal lithosomes, North Carolina, USA. Quaternary Research 69, 97-109.

Mallinson, D., Mahan, S., Moore, C., 2008b. High Resolution Shallow Geologic Characterization of a Late Pleistocene Eolian Environment Using Ground Penetrating Radar and Optically Stimulated Luminescence Techniques: North Carolina, USA. Southeastern Geology 45 (3), 161-177.

Mallinson, D.J., Smith, C.W., Culver, S.J., Riggs, S.R., Ames, D., 2010. Geological characteristics and spatial distribution of paleo-inlet channels beneath the outer banks barrier islands, North Carolina, USA. Estuarine, Coastal and Shelf Science.

McNeill, D.F., 1985. Coastal Geology and the Occurrence of Beachrock: Central Florida Atlantic Coast. In: Stauble, D.K., McNeill, D.F. (Eds.), Coastal Geology and the Occurrence of Beachrock: Central Florida Atlantic Coast. The Geological Society of America Guidebook for Field Trip #4, 1-27.

Murray, A.S., Wintle A. G., 2000. Luminescence dating of quartz using an improved single-aliquot regenerative-dose procedure. Radiation Measurements 32, 57-73.

Murray MR, 2002. Is laser particle determination possible for carbonate-rich lake sediments? J Paleolimnol 27:173–183.

Murray-Wallace, C.V., Banerjee, D., Bourman, R.P., Olley, J.M., Brooke, B.P., 2002.Optically stimulated luminescence dating of Holocene relict foredunes, Guichen Bay, South Australia. Quaternary Science Review 21, 1077-1086.

Osmond, J.L.; May, J.P., and Tanner, W.F., 1970. Age of the Cape Kennedy barrier-and-lagoon complex. Journal of Geophysical Research 75, 469–479.

Potter, E., Esat, T., Schellmann, G., Radtke, U., Lambeck, K., McCulloch, M., 2004. Suborbital-period sea-level oscillations during marine isotope substages 5a and 5c. Earth and Planetary Science Letters 225, 191-204.

Potter, E., Lambeck, K., 2004. Reconciliation of sea-level observations in the Western North Atlantic during the last glacial cycle. Earth and Planetary Science Letters

217, 171-181.

Prescott, J.R., Hutton, J.T., 1988. Cosmic ray and gamma ray dosimetry for TL and ESR. Nuclear Tracks and Radiation Measurements 14, 223–227.

Reinson, G.E., 1992. Transgressive barrier island and estuarine systems. In: Walker, R.G., James, N.P. (Eds.), Facies Models: Response to Sea-level Changes. Geologic Association of Canada, Ontario, pp. 179-194.

Rink, W.J., Odom, A.L., 1991. Natural alpha recoil particle radiation and ionizing radiation sensitivities in quartz detected with EPR: implication for geochronometry. Nuclear Tracks and Radiation Measurements 18, 163–173.

Rink, W.J., Forrest, B., 2005. Dating evidence for the accretion history of beach ridges on Cape Canaveral and Merritt Island, Florida, USA. Journal of Coastal Research 21 (5), 1000-1008.

Robert, R.G., Galbraith, R.F (In Press). Statistical aspects of equivalent dose and error calculation. In Krbetschek, M. (Ed) Luminescence Dating: An Introduction and Handbook, Chapter 7, 23p. Berlin: Springer.

Schmalzer, P.A., Hinkle, C.R., 1990 Geology, Geohydrology and Soils of Kennedy Space Center, Florida. NASA Technical Memorandum 103813, 52 p.

Schulmeister, M.K., Butler, J.J., Healey, J.M., Zheng, L., Wysocki, D.A., McCall, G.W., 2003. Direct-Push Electrical Conductivity Logging for High-Resolution Hydrostatigraphic Characterization. Ground Water Monitoring and Remediation 23, 52-62.

Smith, D.G., Jol, H.M., 1995. Ground penetrating radar: antenna frequencies and maximum probable depth of penetration in Quaternary sediments. Journal of Applied Geophysics 33, 93-100.

Stokes, S., 1999. Luminescence dating applications in geomorphological research.Geomorphology 29, 153-171.

Susman, K.R. and Heron, S.D., Jr., 1979. Evolution of a barrier island, Shackleford Banks, Carteret County, North Carolina. Geological Society of America Bulletin 90, 205-215.

Tatumi, S.H., Kowata, E.A., Gozzi, G., Kassab, L.R.P., Suguio, K., Barreto, A.M.F., Bezerra, L.P.R., 2003. Optical dating results of beachrock, eolic dunes and sediments applied to sea-level changes study. Journal of Luminescence 102-103, 562-565.

Thompson, J., Rink, W.J., Lopez, G.I., 2007. Optically stimulated luminescence age of the Old Cedar midden, St. Joseph Peninsula State Park, Florida. Quaternary Geochronology 2, 350-355.

van Heteren, S., Fitzgerald, D.M., McKinlay, P.A., 1994. Application of Ground Penetrating Radar in Coastal Stratigraphic Studies. Northeastern Section Meeting, Geological Society of America 26, 869-881.

Wintle, A.G., 2008. Fifty years of luminescence dating. Archaeometry 50, 276-312.

SOUTHEASTERN GEOLOGY
V. 47, No. 4, November 2010, p. 191-206

CORRELATION OF THE SANDERSVILLE LIMESTONE LITHOFACIES TO THE OCMULGEE FORMATION, GEORGIA COASTAL

JOHN R. ANDERSON

Science Department, Georgia Perimeter College, 3251 Panthersville Road, Decatur, GA, 30034, john.anderson@gpc.edu, FAX 678-891-2961

CHERYL GULLETT-YOUNG

Benjamin E. Mays High School, 3450 Benjamin E Mays Dr SW, Atlanta, GA 30331, cdyoung@atlanta.k12.ga.us, FAX 404- 699-6781.

W. CRAWFORD ELLIOTT

Department of Geosciences, Georgia State University, Atlanta, GA 30302-4105, wcelliott@gsu.edu, FAX 404-413-5768

ABSTRACT

The Sandersville Limestone Member of the Tobacco Road Sand is a thin (< 6 m), compact, cream to white-colored fossiliferous limestone containing small (<2 cm diameter) clay and chert nodules. The Sandersville Member is middle Jacksonian (Eocene) in age based on the presence of prominent index fossils such as: the echinoid, *Periarchus quinquefarius*; the giant oyster *Crassostrea gigantissima;* and, the bryozoa species, *Crisia edwardsi*, *Perigastrella rhomboidalis*, and *Spiropora majuscula*. Based on the presence of one or more characteristic facies for Eocene rocks in the Atlantic Coastal Plain, per Harris et al. (1997), the Sandersville Member is correlated lithostratigraphically from its type locality in Washington County to facies within the Ocmulgee Formation of central Georgia and to facies within a silicious section in eastern Georgia near Louisville.

The Sandersville Limestone Member has undergone various diagenetic processes since deposition. These processes include: dissolution, silicification, and precipitation of iron phases by iron fixing bacteria. Overall, the deposition of the Sandersville Member shows a deepening of the depositional environment from a calm shelf to a deeper marine shelf with pelagic organisms. This finding correlates with the late Eocene global warming and an increase in sea level due to eustatic sea level rise.

INTRODUCTION

The Sandersville Limestone Member of the Tobacco Road Sand is a thin (< 6 m), compact, white to cream-colored, fossiliferous limestone containing small clasts (<2 cm diameter) of chert, micrite, and silicate clay. The Sandersville Limestone Member is found in only a few locations in central and east-central Georgia (Pierson, 1951; Huddleston and Hetrick, 1986; Foote et al., 2003). It was first described by Veatch and Stephenson (1911), who considered it to be part of the Claiborne McBean Formation. Cooke and Shearer (1918) revised this classification, placing the facies in the upper part of the Barnwell Formation. Cooke (1943) named this unit the Sandersville Limestone Member of the Barnwell Formation. Huddlestun and Hetrick (1986) consider the Sandersville Limestone to be a member of the Jacksonian Tobacco Road Sand, a part of the Barnwell Group first described by LaMoreaux (1946a; b) which represents a shallow marine environment during the Jacksonian Stage of the Eocene Epoch.

The type locality of the Sandersville Member is located 1.3 kilometers south of the Washington County courthouse in Sandersville, Georgia (Huddlestun and Hetrick, 1978; 1986). Notably, the Sandersville Limestone Member contains numerous marine fossils, including ostracods,

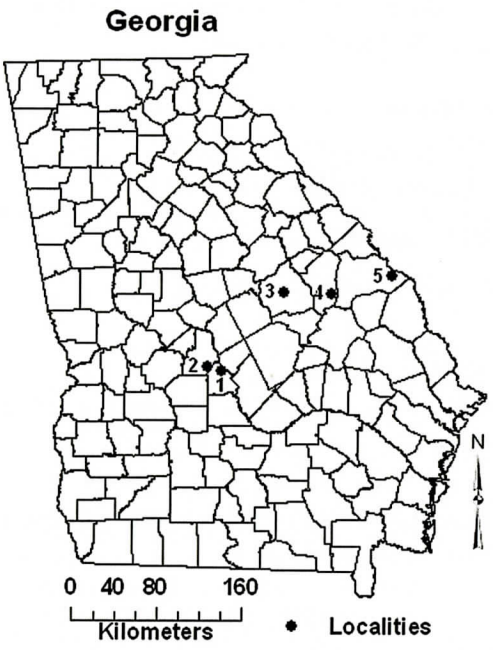

Figure 1. Map showing location of Sandersville Limestone and Ocmulgee Formation collecting localities. 1. Type locality of the Ocmulgee Formation exposed at Taylors Bluff on the Ocmulgee River, Pulaski County, GA; 2. Locality of the Ocmulgee Limestone along U.S. 341 southeast of Haynesville, GA ; 3. Type locality and locations close to the type locality off of Saffold Road, south of Sandersville, Washington County, GA, and in the Tennile Lime sinks, south of Sandersville, GA; 4. Exposure of the silicified Sandersville Limestone along Spring Creek, 13.4 kilometers southeast of Louisville, Jefferson County, GA along GA 17; 5. Core sample of the Barnwell Formation from the core drilled near Girard, Burke County, GA.

mollusks, bryozoa, the echinoid index fossil, *Periarchus quinquefarius* and the giant oyster *Crassostrea gigantissima* (Dowling et al, 2000; Pajewski et al., 2000; Foote et al., 2003). Biostratigraphic studies place the Sandersville Member in the Middle Jacksonian, dating to about 38 million years ago (Young et al., 2003; Foote et al., 2003; Suurmeyer et al., 2003; Wortman et al., 2004). In addition, varying amounts of fine to medium grained sand, clay clasts, and glauconite grains are interspersed within this limestone. The clay clasts contain smectite and quartz.

The study of the Sandersville Member and the underlying Twiggs Clay provides insight into Eocene paleogeography as well as the diagenetic processes affecting these strata. Such changes potentially take place within both the underlying Twiggs Clay and the world-class kaolin deposits of late Cretaceous-Early Tertiary age (Pickering et al., 1997; Hurst and Pickering, 1997; Kogel et al., 2000). The biostratigraphic results discussed herein permit the lithologic correlation of the Sandersville Member to the Ocmulgee Formation of the west-central Georgia coastal plain near Macon, and to the Barnwell Formation of the eastern Georgia coastal plain near Augusta.

METHODS

The lithology of the Sandersville Limestone Member, the Ocumulgee Limestone, and the Barnwell Formation were described both macroscopically from hand specimens as well as petrographically using thin sections. The Sandersville Limestone was collected from three localities in Washington County, GA: the Tennile Limesinks, an exposure of the limestone in the stream bed off of Saffold Road, and the type locality on the southern edge of Sandersville, Georgia, (Location 3, Figure 1)(Anderson et al., 1999). Additionally, an outcrop of silicified Sandersville Limestone was found along the banks of Spring Creek southeast of Louisville, Georgia, along Georgia State Road 17 (location 4, Figure 1) (Pierson, 1951). Limestone strata believed to be equivalent to the Sandersville Limestone Member were observed in core of the Upper Three Runs Aquifer, Barnwell Formation, drilled near Girard, Georgia, in Burke County (location 5, Figure 1).

The Ocmulgee Limestone was analyzed in this study at its type locality along the banks of the Ocmulgee River north of Hawkinsville, Georgia, where it is underlain by the Twiggs Clay Member of the Dry Branch Formation and is overlain by the Ocala Formation (a similar limestone unit to the Ocmulgee Formation) (Location 1, Figure 1). To the north and east of the type locality, it is overlain by the Tobacco

Table 1. Faunal List

Fossils	Ocmulgee	Sandersville	Louisville	Girard core
Foraminifera				
Bolivina sp	X			
Camerina jacksonensis		X		
Cibicides sp.		X		
Cibicides zitteli	X			X
Clavulinoides sp.	X			
Dentalia sp.	X			
Dentalia cooperensis	X			
Elphidium sp.	X			
Globigerina sp.	X			
Globorotalia sp.	X			
Globorotallia velascoensis	X			
Gumbelina globulosa	X			
Valvulineria jacksonensis		X		
Coral				
Flabellum cuneiforme	X	X		
Bryozoa				
Beisselina sp.	X			
Berenicea benjamini			X	
Cellaria bifactata	X			
Chelostomatous sp.	X			
Crisiae edwards	X			
Diaperocia varians		X		
Erksonea admota		X		
Erksonea parkeri		X		
Idmonea magnireversum	X	X		
Lunulites jacksonensis	X	X		
Lunulites distans		X		
Membraniporia laxa		X		
Membraniporia trigemma	X			X
Membraniporidra spissimuralis	X			
Metrocopulsa sp.	X			
Ochetosella jacksonica	X			X
Perigastrella rhomboidalis	X			
Plagiocia concerta	X		X	
Polyascosecia jacksonica	X			
Schizomavella granulifera	X			X
Spiropora majuscula	X	X		
Stamenocella antina				X

Fossils	Ocmulgee	Sandersville	Louisville	Girard core
Mollusks				
Bivalves				
Assorted pieces	X	X		X
Pectins	X	X		
Gastropods	X	X		
Turritella sp.		X		
Mitra sp.		X		
Phalum sp.		X		
Scaphopods	X	X		
Arthropods				
Decapod claws	X			
Barnacle plates	X	X		X
Ostracod				
Aulocytheridea mangodentata	X			
Brachycythere gigantean	X			
Cuneocythere sp.		X		
Cypria sp.		X		
Cytherella sp	X			X
Cytherella alexanderi	X			
Cytherelloidea ocalana	X			
Spongicythere willistonensi	X			
Trachyleberis citrusensis	X			
Echinoderms				
Echinoid spines & plates	X	X	X	X
Periarchus quinquefarius	X	X	X	
Ophiuroid plates	X	X	X	X
Vertebrates				
Fish Teeth	X	X		X
Shark Teeth	X	X		
Skate Teeth		X		
Manatee ribs & vertebrae		X		
Sea Turtle vertebrae		X		

Road Sand Formation in central and eastern Georgia. The thickness of this formation ranges from 2.5 to 5.8 meters and it extends from Houston and Pulaski Counties in west-central Georgia to areas along the Savannah River at the Georgia – South Carolina state border. The Ocmulgee Limestone was also collected from an outcrop along U.S. 341 southeast of Haynesville, Georgia (location 2, Figure 1) (Suurmeyer et al., 2003; Wortman et al., 2004; Stephens et al., 2007). The Barnwell Formation was collected from a drill core in Girard County (Clarke et al., 1994; Clarke et al., 1996; Falls and Prowell, 2001; Edwards et al., 2001).

Insoluble residues were produced by dissolving the limestone at room temperature with either a 1 N hydrochloric acid solution or with a 1 N or a 5 N sodium acetate-acetic acid buffer at 4.5 pH (Jackson, 1985). The sand insoluble fractions were examined using a stereomicroscope under low magnifications (10x). The mineral compositions of the sand fraction and the clay and fine silt fraction were determined using both visual examination and X-ray diffractometry. Oriented mounts of the clay fraction and random mounts of the coarser insoluble residues were scanned at a rate of 1^{o} 2θ per minute using copper radiation produced at 35 kilovolts and 15 milliamperes and filtered with a graphite monochromator. An MDI Databox® was used for scanning, acquisition, and plotting diffraction data. The clay fractions were also solvated in ethylene glycol to identify smectite (Moore and Reynolds, 1997).

The fossils were extracted from the limestone by boiling the rock in a solution of Amine Q-O; the fossils were picked from the residue using a stereoscopic microscope. The fossils found in the Sandersville Limestone Member, Ocmulgee Limestone, and Barnwell Formation were identified and their geological ranges were plotted to derive a biostratigraphic age for this unit and lithostratigraphic correlation.

RESULTS

Paleontology

The fossils observed in the Sandersville Limestone Member, Ocmulgee Formation and in the Barnwell Formation of the Girard core are listed in Table 1. The Sandersville Limestone Member contains a diverse assemblage of marine bryozoa, foraminifera, mollusks, echinoderms, fish teeth, shark teeth, ray teeth, and various marine vertebrates. Likewise, the Ocmulgee Formation contains a diverse assemblage of bryozoa, gastropods, echinoderms, ostracods, brachiopods, foraminifera and fish teeth in the lower part whereas the upper part of the Ocmulgee Formation is more calcareous and contains deeper marine fauna such as foraminifera and ostracods. The stratigraphic range for the fossils observed in the Ocmulgee Formation and the Sandersville Limestone Member are shown in Figures 2 and 3. The Barnwell Formation contains fragments of abraded bivalves, gastropods, and bryozoa including *Ochetosella jacksonica*. The echinoid *Periarchus quinquefarius* was found in all the exposures of the Sandersville Limestone Member, the Ocmulgee Formation and the silicified Sandersville at Louisville, Ga. (Table 1).

Petrology

Ocmulgee Formation

The Ocmulgee varies from a carbonate cemented quartz sandstone at its base to a limestone at the uppermost part of the outcrop at the type locality. Table 2 shows the results of abundance estimates for the framework grains, matrix, cement, and pore types for the Ocmulgee Formation. Smectite, angular glass shards, and small amounts of glauconite grains are present in the clay fractions of the insoluble residues. The shards contain Si and Al and are altered to zeolites, smectites and opal-CT, based on X-ray diffraction (Stephens et al., 2005). Glauconite grains are found as discrete botryoidal dark green grains in the Ocmulgee Formation at 6.0 - 6.7 meters above the basal contact whose K-Ar dates and mineralogy are described in Stephens et al. (2007). Five facies are recognized based on thin section study of the Ocmulgee Formation at its type locality (Figure 2). These five facies are correlative to facies noted by Harris et al. (1997); they are, from base to top

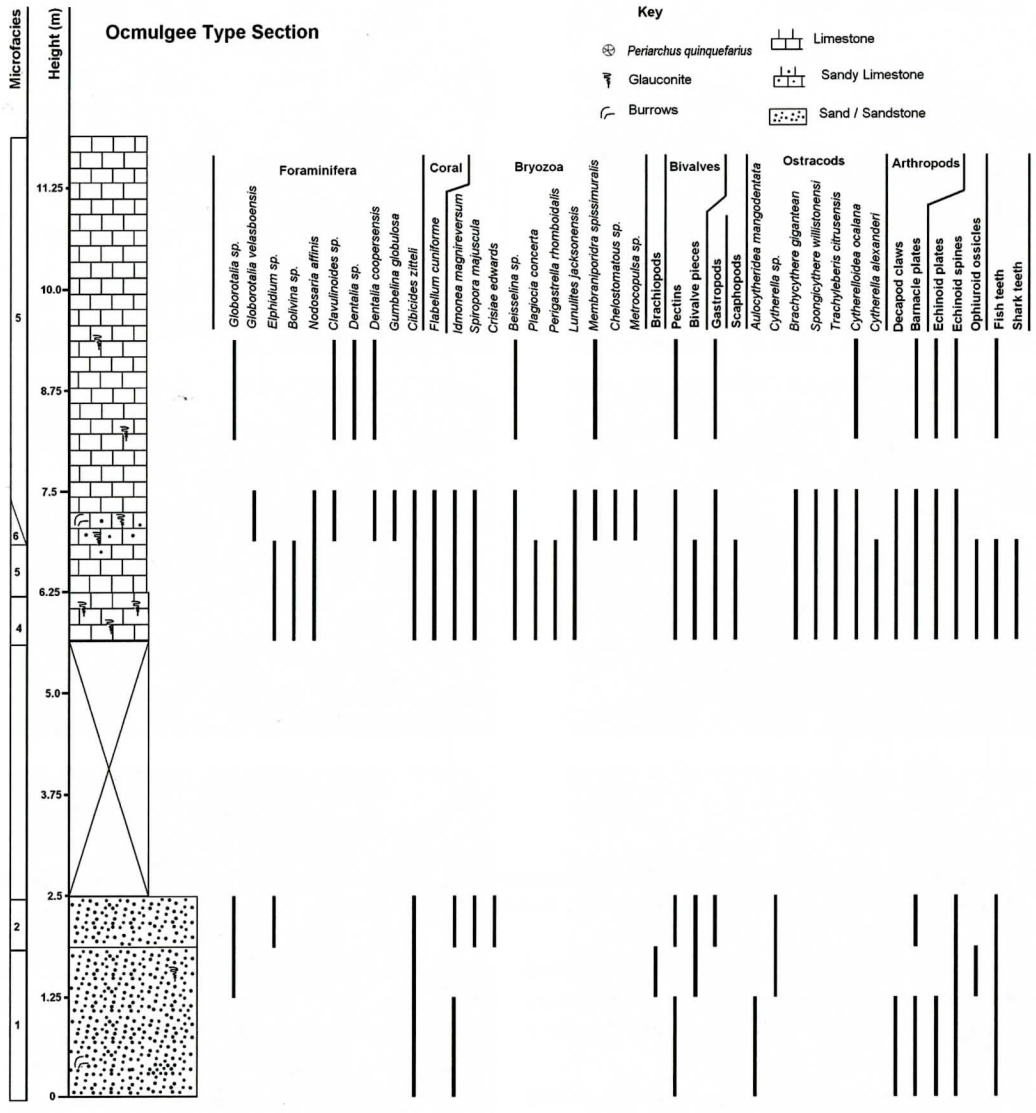

Figure 2. Stratigraphic Section of the Ocmulgee Formation showing microfacies observed and stratigraphic range of fossils found within this unit.

[numbers represent the microfacies numbers used by Harris et al., (1997) within their study]: (1) quartz sand, (2) skeletal quartz sand, (4) skeletal wackestone and quartz-rich skeletal wackestone, (5) skeletal packstone and quartz-rich skeletal packstone, and (6) quartz-rich, glauconitic wackestone-packstone. These facies are described below for the Ocmulgee Formation at the type location where we make note of our petrographic, paleontologic, and mineralogic data.

Quartz sand: This facies is 1.8 meters thick. It is a structureless fine-grained sand with angular to subangular grains (Figure 4A). Microspar is the primary cement that has been dissolved in some areas to form interparticle and vug porosity. There are thin veins of unconsolidated detrital quartz that have been loosely cemented with neomorphic spar. A diverse fauna is found in this facies (foraminifera, echinoderms, bryozoa, gastropods, ostracods and bivalves). The abundances of these fauna are low. These fos-

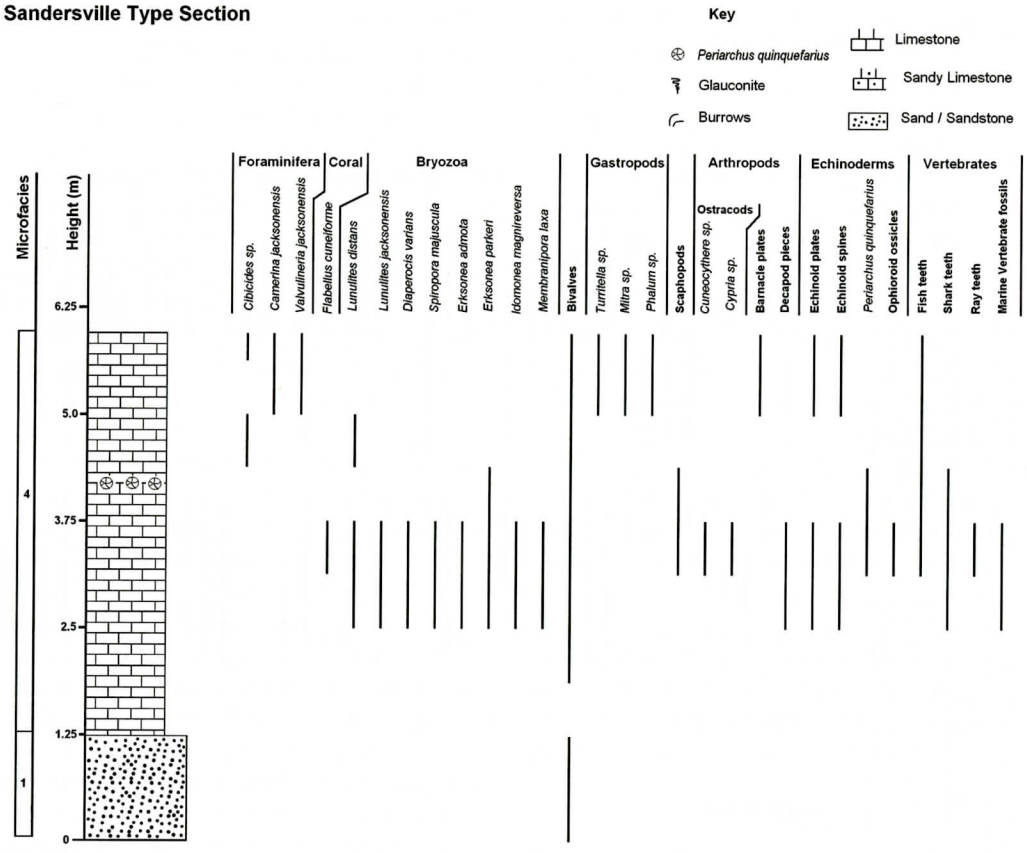

Figure 3. Stratigraphic Section of the Sandersville Limestone Member showing microfacies observed and stratigraphic range of fossils found within this unit.

sils are rounded and broken and some have sand grains surrounding them on all sides. Phosphate and glauconite grains are present in trace amounts.

Skeletal quartz sand: The skeletal quartz sand begins at 1.8 meters above the base and it is 0.6 meters thick. It is also a weakly consolidated fine-grained sand with angular to sub-angular grains and microspar cement (Figure 4B). This facies has variable porosity ranging from highly porous to very low porosity relative to the underlying quartz sand. The low porosity, when examined in hand specimen, resembles an intraclast of micrite, but in thin section it is a very dense and pure microspar with little or no framework grains that grades into the higher porosity microspar (Figure 4B). Pores are largely interparticle but molds and vugs are also present. Fossil diversity is the same as for the quartz sand facies but a higher abundance of fossils, especially foraminifera, echinoderms, and bryozoa, occurs in this facies. These fossils are also broken and rounded with some showing signs of micritization and algal borings.

Skeletal wackestone: Skeletal wackestone is found in a 0.6 meter interval 2.5 meters above the base. Detrital quartz is present in small amounts that range from fine to medium grained. The cement is a microspar and in some places fringing blocky calcite spar outlines moldic and vuggy pores or replace bivalve shells. Glauconite grains are abundant and occur as iron stained pellets. A fine-grained glauconite replaces bryozoan zooecia. This facies, like the skeletal quartz sand, has a diverse fauna dominated by foraminifera and ostracods. Echinoderms, bryozoa, gastropods, and bivalves are less abundant.

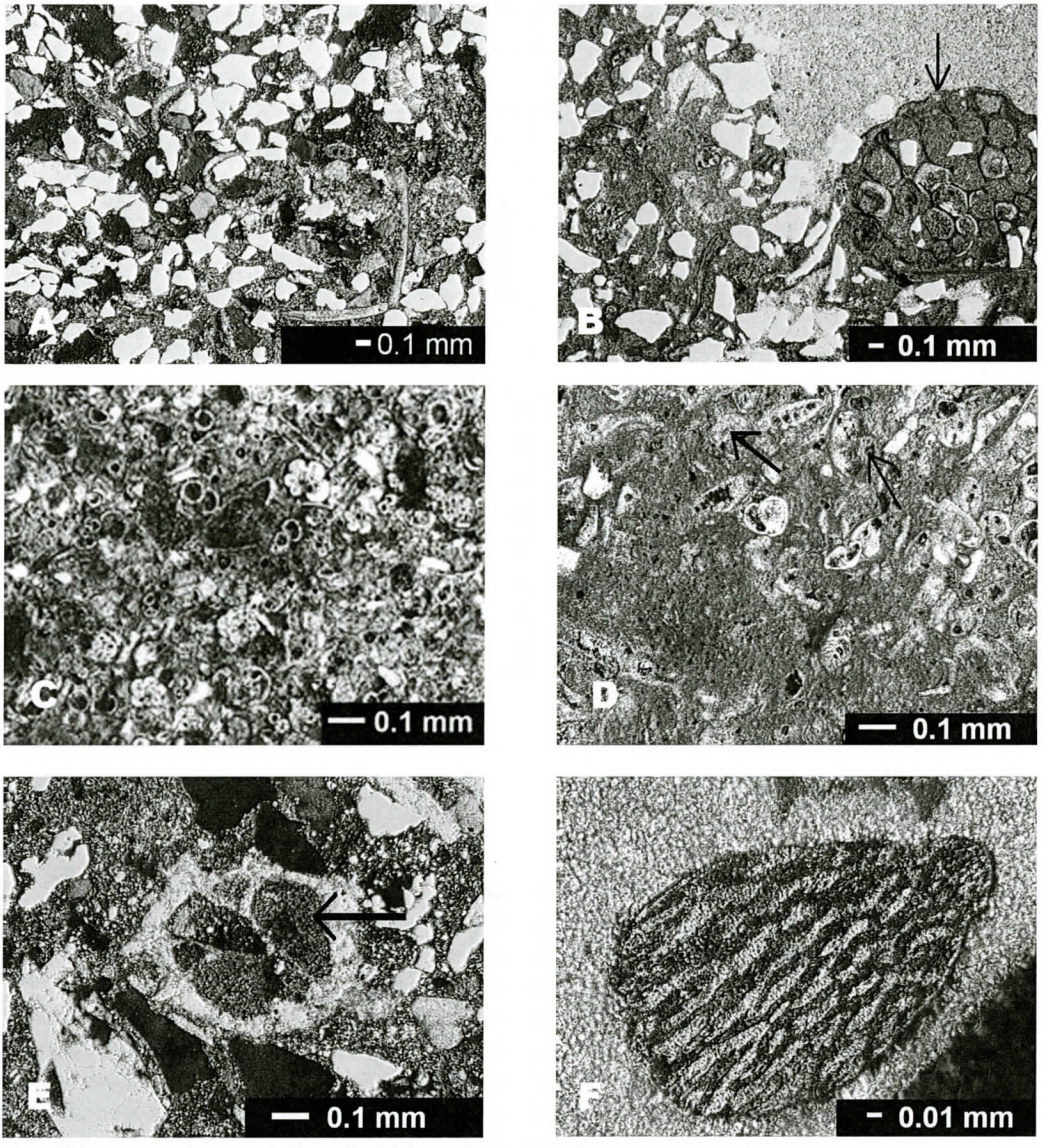

Figure 4. Photomicrographs showing: A) Quartz Sand with microspar matrix and rounded bioclasts. Sample # OKG-002. B) Skeletal quartz sand with the interface between a porous zone, in lower left of photomicrograph and low porosity zone in the upper right of photomicrograph. Arrow points to the bryozoa zooarium, Sample # OKG-003. C) Skeletal packstone containing abundant ostracods and foraminifera within a microspar matrix. Sample # OKG-006. D) Skeletal packstone at the top of the photomicrograph with well developed secondary porosity (arrows). The lower portion of the photomicrograph shows an unaltered micrite matrix. Foraminifera and ostracod skeletons characterize this microfacies. Sample # OKG-009. E) Quartz-rich glauconitic wackestone. Glauconite (arrow) fills the interior of gastropod shell. Sample # OKG-009. F) Glauconite pellet within micrite matrix. Sample # OKG-005. All photomicrographs from the Ocmulgee type locality.

TABLE 2. Composition of Ocmulgee Formation at its type locality in Georgia.

Meters above Twiggs Clay	Microfacies	Framework Grains								Matrix	Cement		Pore Types			
		Quartz	Bivalves	Gastropods	Foraminifera	Bryozoa	Echinoderms	Ostracods	Phosphate/Glauconite	Micrite	Neomorphic Spar	Calcite Spar	Interparticles	Intraparticles	Moldic	Vugs
8.5 – 9.1	5	T			A			A	T	A			C	R		
7.3 – 7.9	5	T			A			A	R	C	A	R	R			
6.7 – 7.3	5/6	R			A	T	R	A	C		A		R	R		R
6.7 – 7.3	5	T	T		A	R	R	A	R		A		C	C		
5.5 – 6.0	4	R	T	T	C	R	R	C	C		A	R	T	T	C	R
1.8 – 2.4	2	A	R	T	R	R	R	T	R		A		R	R	R	T
1.2 – 1.8	1	A	T	T	R	R	T	T	T		A		R	R	R	R
0.6 – 1.2	1	A	T	T	T	T	T	T	T		A		R	T		R

A = Abundant (>25%)

C = Common (<25%, >10%

R = Rare (<10%)

T = Trace (<1%)

The section between this facies and the overlying facies (3–5.5 m above base) is presently covered with vegetation. In an earlier study, Huddlestun and Hetrick (1986) described this part of the section from 3–5.5 m above the base as composed of a "soft, slightly glauconitic.... fossiliferous with abundant molluscan molds" limestone. Their description of this covered part of the section is similar to the description of the skeletal wackestone facies.

Skeletal packstone: A skeletal packstone is found in an 5.5 meter interval from 6 meters to the top of the section at 11.5 meters above the base of the unit at the type locality. This facies contains well-sorted ostracod and foraminifera bioclasts (Figure 4C). Detrital quartz grains are rare, well-rounded, and silt sized. The matrix/cement ranges from microspar at the base of the skeletal packstone to micrite at the top. In between, there are varying amounts of microspar and micrite. The micrite usually appears as small peloids (Figure 4C). In one layer, sparry calcite is the dominant cement filling many of the pores. This sparry calcite cement contains micrite nodules. This section, except for the calcite spar layer, is very porous. Most of the porosity is interparticle. The fossils in this section are primarily foraminifera and ostracods with trace amounts of bivalves and echinoderms (Figure 4D). This section marks the appearance of globorotalid foraminifera, the most abundant type of foraminifera within this part of the section. A quartz-rich glauconitic wackestone occurs 6.7–7.3 m above the base and is further described below.

Quartz-rich glauconitic wackestone: This microfacies is found within the skeletal packstone approximately 6.7–7.3 m above the base of the section. Detrital quartz is angular and medium grained (Figure 4E). Glauconite is in the form of pellets or rounded grains (Figure 4F). All glauconite grains have cracks and show oxidation. The matrix is microspar with minor calcite spar cement. In general, the facies is

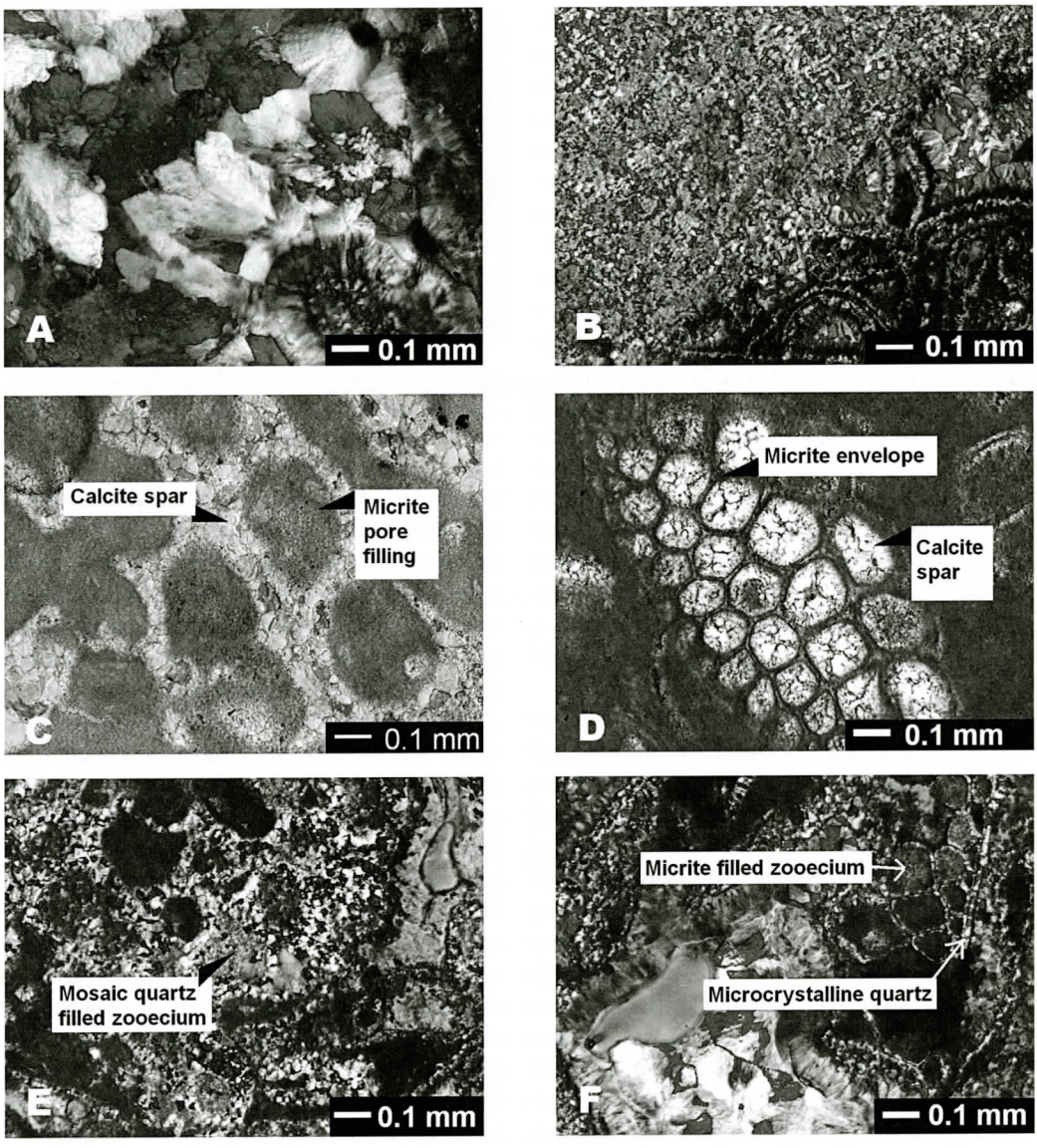

Figure 5. Photomicrographs showing A) The pore center shows mosaic quartz forming adjacent to chalcedony from Spring Creek locality of the Sandersville Member. B) Photomicrograph showing recrystallized area containing microcrystalline quartz. The typical sample matrix is exhibited at the bottom right. C) Bryozoa from the Sandersville Limestone at the Tennile Lime Sink locality showing calcite spar skeletal replacement and micrite pore filling. D) Bryozoa from the Sandersville Limestone at the Tennile Lime Sink locality showing micrite skeletal structure and calcite spar infilling the zooecium. E) Bryozoa from the silicified Sandersville Limestone at the Spring Creek locality showing microcrystalline quartz within the zooecium of the bryozoa. F) Bryozoa from Spring Creek locality of the silicified Sandersville Limestone showing micrite filled zooecium and microcrystalline quartz replacement of the skeletal wall.

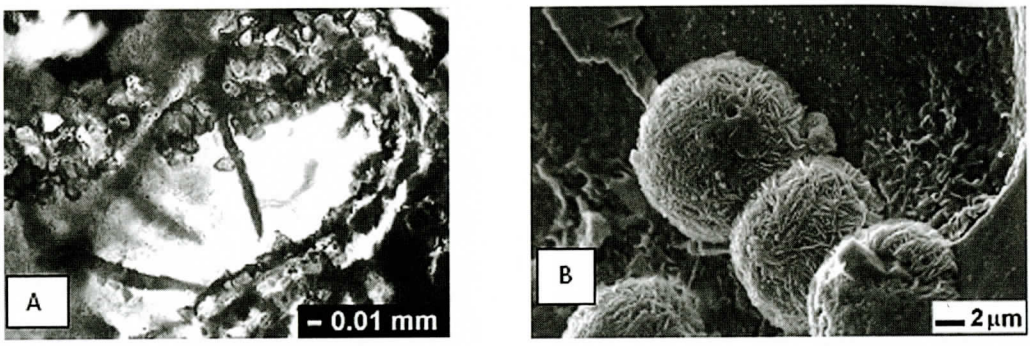

Figure 6. Photomicrographs showing A) Interpreted bacteria filaments in fringing chalcedony. Notice the quartz overgrowth on the filaments in the center. B) Glass shard altered to zeolite, smectite and opal-CT.

porous. Most of the porosity is interparticle or vuggy. Some of the pores are moldic of bivalve or brachiopod shells. Fossils are primarily foraminifera (especially globorotalids) and ostracods, with a trace of fragmented bivalves.

Sandersville Limestone Member, Sandersville, Georgia

The Sandersville Limestone Member is a friable, fossiliferous micrite containing lesser sparry calcite limestone with abundant shell fragments. Sparry calcite also fills dissolution cavities in this limestone. The insoluble residues are composed of quartz, feldspar, and clay clasts. Feldspars exist as clayey pseudomorphic clasts. Smectite, kaolinite, illite, and halloysite are found in the clay fractions of the Sandersville Limestone. As in the Ocmulgee Formation, angular glass shards containing Al and Si are present in the Sandersville Member.

Of the seven microfacies given by Harris et al. (1997) for Eocene rocks in the Atlantic Coastal Plain, only two of these facies appear in the Sandersville Member. These are: (1) quartz sand, and (2) skeletal wackestone and/or quartz-rich skeletal wackestone. The skeletal wackestone facies has qualities that do not entirely match the characteristics described by Harris et al. (1997). The Sandersville Limestone Member has higher percentages of bivalves than Harris et al. (1997) found in their wackestone facies; there is a much lower percentage of foraminifera in the Sandersville than what Harris et al. (1997) found within their wackestone. Overall the Sandersville section is well indurated at its base and is a more friable, carbonate-rich lithology towards the top. There is evidence of secondary porosity of the Sandersville Member in the upper 2.5 meters of the unit. Recrystallization and localized silicification are evident throughout this unit.

Quartz sand: This facies is found at the base of the section and is 1.2 m thick. It is a fine-grained, subangular to subrounded sand. Micrite is the cementing phase. Fossils are rare. Bivalve and bryozoa are present near the contact with the overlying skeletal wackestone. Phosphate and glauconite are present in trace amounts.

Skeletal wackestone: The skeletal wackestone facies is fairly uniform for most of the 5.8 m of exposure above the quartz sand facies. The cement is microspar, or in some places is blocky calcite spar that appears on the edges of moldic and vug pores or replaces fossils (usually bivalve shells). Glauconite is rare and is found in pellet form with iron oxide staining, or it replaces bryozoan zooecia. Fossils include echinoderms, gastropods, foraminifera, and ostracods, but the most common fossils are bryozoa and bivalves. A quartz-rich skeletal wackestone composed of fine to medium grained detrital quartz is found at the upper 1.2 m of exposure.

Sandersville Member, Spring Creek.

At the Spring Creek locality, the Sandersville Limestone Member is a silicified, poorly-washed, biosparite (Folk, 1962). The facies de-

fined by Harris et al. (1997) are not identified in this section. The Sandersville Member is distinct here because of the presence of silica cementation as opposed to carbonate cements present at the other locations. Three cements are observed in the Spring Creek section: chalcedonic overlays; spherulitic chalcedony, and microcrystalline, and mosaic quartz. In addition to the cements, three distinct quartz crystal morphologies are observed in the larger pores, those approximately 15 μm in diameter. The interior of the pore structure is made up of a fibrous chalcedonic overlay followed by length-fast, the stacking orientation, perpendicular to c-axis, of the microcrystals, spherulitic chalcedony juxtaposed to a length-slow, stacked along the c-axis, quartzine in the center of the structure. When viewed in plane polarized light, the chalcedonic overlay has iron oxide laminae (Figure 5A). The larger pores (45 μm in diameter) contain blocky mosaic quartz in the center of the pore enclosed by spherulitic chalcedony (Figure 5A). The shells of skeletal fragments which form the framework of the Sandersville Limestone Member are typically composed of uniform microcrystalline quartz. In many cases, quartz overgrowths fringe fossil fragments and reduce primary porosity. Porosity within the skeletal fragments, such as the interiors of bivalves or chambers within gastropods, is highly variable. Some pores are fully reduced whereas others show only minimal cementation by silica. Several structures were observed that exhibit a pore reduction followed by dissolution. In addition to being present as a shell replacement, microcrystalline quartz occurs in the micritic matrix. In areas which had partially filled and open pores, the quartz is stained by iron oxides (Figure 5B).

Bryozoa were analyzed to determine the fabrics before and after silicification. Calcite structures in the Sandersville Member were compared to the silicified structures at the Spring Creek locality. At the Tennile Lime Sinks, bryozoa found in the Sandersville were recrystallized, with calcite spar replacing the shell material. Internal detail varies based on the method of replacement. In some bryozoa the zooarium, the entire bryozoans colonial skeleton, recrystallized to sparry calcite and the void space, the zooecium, the tube or chamber of the colony, also known as autopore, was filled primarily with micritic mud (Figure 5C). In other thin sections the zooecia are filled with sparry calcite, and micrite envelops the skeleton, the zooarium (Figure 5D). In thin sections from the Spring Creek locality, where the limestone has been silicified, the bryozoa show patterns of recrystallization of the zooarium and zooecium similar to what was observed in the unsilicified Sandersville Limestone. In Figure 5F the zooarium is filled with "sparry" quartz and the zooecium is filled with microcrystalline (what would have been micrite) quartz as observed in Figure 5C of the Sandersville Limestone. Figure 5E shows microcrystalline quartz enveloping the zooarium with some of the zooecia filled with mosaic quartz similar to sparry calcite, as observed in Figure 5D of the Sandersville Limestone.

Bacteria filaments were also observed within the silicified Sandersville Limestone at the Spring Creek locality. The bacteria filaments are fringed with chalcedony and display overgrowths of quartz (Figure 6A).

Barnwell Formation, from drill core:

The Barnwell Formation is a skeletal wackestone containing calcite, quartz, and fossil fragments (bivalves, gastropods, and bryozoa), based on examination of drill core. As in the Ocmulgee Formation and Sandersville Limestone Member, quartz and small amounts of clay are present in the insoluble residues. The fine fractions contain angular glass shards. The clay fractions of the Barnwell Formation contain heulandite, smectite, opal CT; the angular glass shards contain Ti as well as Si and Al (Figure 6B).

INTERPRETATION AND DISCUSSION

Diagenesis and Stratigraphy

The presence of correlative index fossils and the skeletal wackestone with a mud matrix permits a time-stratigraphic correlation from the

Table 3. Geological distribution of fossils found in the Sandersville and Ocmulgee marine units.

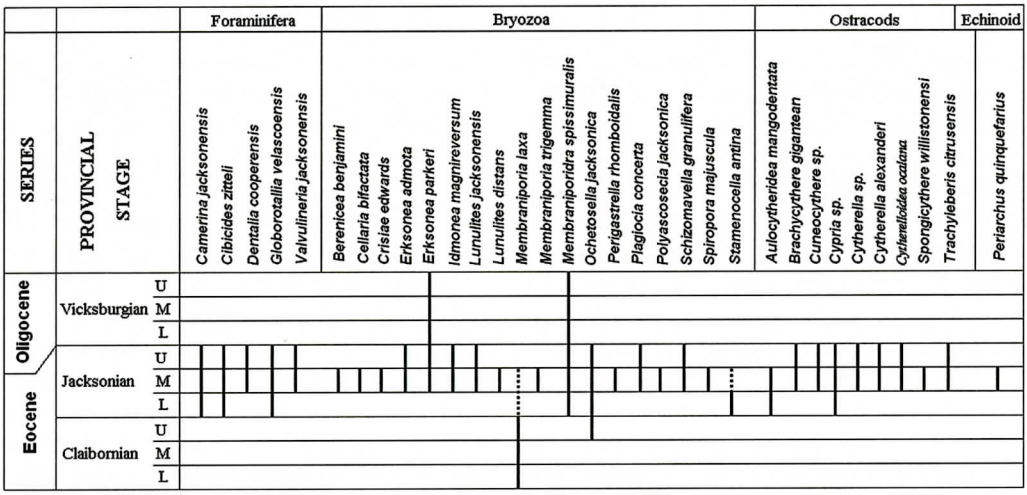

Sandersville Member to the Ocmulgee Formation. In particular, the most notable index fossil found in both the Sandersville and the Ocmulgee is the echinoid *Periarchus quinquefarius*, which is a diagnostic index fossil for the Middle Jacksonian Stage of the Upper Eocene strata on the Coastal Plain of Georgia (Pickering, 1970). Other fossils that enable correlation include the bryozoa species *Idmonea magnireversum*, *Lunulites jacksonica*, and *Spiropora majuscula*, and the coral species *Flabellum cuneiforme* (Table 1). The presence of the bryozoa species *Berenicea benjamini*, *Cellaria bifactata*, *Crisiae edwardsi*, *Lunulites distans*, *Membraniporia trigemma*, *Perigastrella rhomboidalis*, *Polyascosecia jacksonica*, and *Spiropora majuscula*, the ostracod species *Spongicythere willistonensi*, and the echinoid species *Periarchus quinquefarius* indicate an age of Middle Jacksonian (Table 3). In addition to the common fossil assemblages between the Ocmulgee Formation and the Sandersville Limestone Member, lithologic correlations are possible between these units based on the presence of the skeletal wackestone and quartz-rich skeletal wackestone facies.

Diagenetic features obscure some of the initial textures as well as some of the fossils present in both the Ocmulgee Formation and the Sandersville Limestone Member. The presence of increased porosity, replacement of fossils by diagenesis, compaction, and in some areas, silicification is typical of these units. These features indicate that both the Ocmulgee Formation and the Sandersville Limestone in Sandersville, Ga., have been affected by diagenetic processes associated with both marine and freshwater phreatic systems. Moreover, the diagenetic processes affecting the lower quartz sand facies are distinct from the diagenetic processes affecting the overlying packstone and wackestone facies in both the Sandersville Limestone Member and the Ocmulgee Formation.

The basal 1.2 to 2.5 meters of the sections are composed of quartz sand and skeletal quartz sand with minor bivalve and foraminifera shells. The quartz sands are highly resistant to siliciclastic diagenetic processes due to their high contents of detrital quartz and the lack of burial. The effects of marine diagenesis are mostly seen in the skeletal framework grains. Bivalve shells and foraminifera were bored after burial by fungi and algae and their shells replaced with micrite. Microspar was precipitated as a cementing agent holding the quartz grains. Tucker and Wright (1990) observed similar features within diagenetically altered carbonates where some shells were completely dissolved leaving only a faint outline of the shell in the matrix. Moldic pores were formed by dissolution of carbonate skele-

tal fragments that had not been destroyed by micritization. Freshwater phreatic waters also affected the micrite matrix, completely converting micrite to microspar (Figure 4A). Harris et al. (1997) observed this conversion of micrite to microspar in fossils from an Eocene carbonate units on the South Carolina Atlantic Coastal Plain. In our observations, almost all of the skeletal grains had either gone through dissolution or neomorphism. A later dissolution event occurred after the neomorphism of the micrite forming vuggy pores.

The upper layers of the section in both the Ocmulgee Formation and Sandersville Limestone Member that are composed of wackestone and packstone have a similar diagenetic history as the lower layers of each, but there are some subtle differences. The presence of both moldic pores or the original shells themselves indicate that marine diagenetic reactions were less prevalent during early diagenesis of these carbonate-bearing rocks. The moldic pores were formed by dissolution of micrite by freshwater diagensis. Aragonite also survived the micritizing process but was dissolved later. Flugel (1982) observed this moldic pore formation within various carbonate rocks due to reaction with freshwater. The micritic peloids in some layers near the top of the section resemble the size and shape of the surrounding foraminifers within the Ocmulgee Formation. These peloids are signs of a brief interval of micritization that may have happened in the upper layers of the section, but not for an extended period of time because many of the foraminiferia are preserved and show no signs of micritization. In the freshwater phreatic zone, diagenetic processes included: dissolution of aragonite shells to form pores, neomorphism of the micrite to microspar, and a later event of dissolution that formed the interparticle porosity common in these rocks, as observed in Figures 4B, 4C, & 4D. Neomorphism varies in some layers with an increase in the original micrite matrix towards the top of the section. This variation of the original micrite matrix shows possible fluctuations in the ground water table over time. A continuous high water table would have shown neomorphism throughout the whole section. However, if the water table had fluctuated the rock matrix exposed in the vadose zone would have remained micrite while the rock matrix below the water table would have been recrystallized.

Silicification of the Spring Creek and Sandersville Limestone Member

The Sandersville Limestone from the Tennile Lime Sinks locality is a packed, fine-grained, wackestone. The presence of this wackestone suggests that it was deposited in a low-energy marine environment with moderate wave action because of the minor shell abrasion observed in the fossils present. Since the allochems in these wackestones show no signs of compaction or distortion, these strata were not buried to appreciable depths to cause further diagenesis. Several fossil fragments also possess micrite envelopes produced by algal borings, a condition supporting the interpretation of an early diagenetic change during shallow burial, very near the sediment-water interface. The correlative of the Sandersville Member at the Spring Creek locality is a silicified packed wackestone that is interpreted to have been deposited in a low-energy marine environment, based on the similar condition of the shell fragments observed in this rock. Unlike the Sandersville at the Tennile Lime Sinks and other localities near Sandersville, GA, fossil fragments were replaced with microcrystalline quartz, then a pore-reducing chalcedony was later introduced by the addition of silica rich ground water. Fringing chalcedony is commonly associated with the phreatic zone (Thiry and Milnes, 1991). Furthermore, what appear to be abundant filaments of iron-fixing bacteria are found within the fringing chalcedony. Contemporary examples of these bacteria, microaerophiles or aerobes, known as *Gallionella ferruginea*, can thrive in a neutral or acidic environment (Anderson & Pedersen, 2003). For energy, the contemporary bacteria oxidize ferrous iron present in groundwater. The presence of these biogenic iron oxide stains during this stage of silicification thus, indicates that the chalcedonic phases were precipitated in neutral or acidic soil solu-

tion. The mosaic quartz found as cement in the specimens represents the final stage of silicification. Because of their size these crystals take the longest to form. They are also the result of precipitation from a silica-weak solution (Thiry and Ribet, 1999).

The diagenetic processes observed in the Spring Creek strata closely resemble the pedogenic and groundwater silcretes described by Thiry and Milnes (1991) in the Stuart Creek Opal Field, South Australia. As in the Spring Creek specimens, residual voids in the Stuart Creek were filled with chalcedony and mosaic quartz and possessed a matrix of microcrystalline quartz. Other similar petrographical structures were observed at Stuart Creek which are similar to those observed in the silicified Sandersville Limestone of the Spring Creek locality.

Sedimentology

Based on the analyses of thin sections, mineralogy, paleontology, and petrology, the Ocmulgee strata and the Sandersville Member represent a deepening water sequence that changed from a near shore to a deep sea shelf environment. The basal facies of quartz sand with abraded and broken bioclasts indicates a high energy, near shore depositional environment either at or around wave base on a beach or delta. The overlying skeletal wackestone with a mud matrix and fossil assemblage, present in both the Ocmulgee and Sandersville Member, represents a lower energy open marine depositional environment such as an open platform area (Flugel, 1982). Harris et al. (1997) noted similar transitions from mixed carbonate clastic strata in Eocene rocks of the South Carolina Atlantic Coastal Plain.

A skeletal packstone rich in foraminifera and ostracods is present in the Ocmulgee Formation above the wackestone, and above what is currently exposed in the Sandersville Member at its type locality. This packstone represents a lower energy depositional environment of a deep marine shelf environment dominated by pelagic organisms (Flugel, 1982). Harris et al. (1997) described a similar relationship for the skeletal packstone which they interpreted to have formed in a deeper water environment.

CONCLUSIONS

The Sandersville Member was correlated, using lithology and fossil evidence, to the skeletal wackestone of the Ocmulgee Formation based on similar lithology and the presence of the index fossil echinoid *Periarchus quinquefarius*. The presence of the bryozoa species *Berenicea benjamini*, *Cellaria bifactata*, *Crisiae edwardsi*, *Lunulites distans*, *Membraniporia trigemma*, *Perigastrella rhomboidalis*, *Polyascosecia jacksonica*, and *Spiropora majuscula*, the ostracod species *Spongicythere willistonensi*, and the echinoid species *Periarchus quinquefarius* defines the depositional age as the middle Jacksonian Stage of the Eocene Epoch (Table 3). These units are also correlated to the Barnwell Formation in the Girard core. We propose that all of these units be called the Sandersville Limestone, due to precedence of the name, and the correlation of these units based on the criteria listed above. Overall, the deposition of the Sandersville Member shows a deepening of the depositional environment from a calm shelf to a deeper marine shelf with pelagic organisms. This finding may give evidence to the late Eocene global warming and increase in sea level due to eustatic sea level rise and the melting of the polar ice caps.

ACKNOWLEDGEMENTS

This project was sponsored by the Atlanta Consortium for Research in the Earth Sciences (ACRES) a Research Experience for Undergraduates (REU) program, which was funded by the National Science Foundation (EAR-9820666 and EAR 0139539) to Pamela C. Burnley (Primary Investigator). We thank Dr. Robert Simmons (Georgia State University, Biology Department) for SEM photos. The authors would also like to thank the reviewers of this paper Dr. Mary K. Harris, and Dr. Paul A Thayer. We wish to acknowledge the students Donald Dowling, George Amanambu, Tameka Wimberly, Jennifer Germano, Kara Pajewski, Sara Tourscher, Jim Foote, Lawrence Wertan,

Brandon White, Elizabeth Elliot, Kanya Rhedrick, Daniel Williams, Elizabeth Howell, Ryan D. Powell, Angie M. Smith, Nathan R. Suurmeyer, Eric Burger, Kristina Lawrie, Elizabeth Stephens, and Santina R. Wortman who participated in the NSF funded ACRES REU; they performed the research that led to this paper.

REFERENCES

Anderson, C. R., and Pedersen, K., 2003, In situ growth of *Gallionella* biofilms and partitioning of lanthanides and actinides between biological material and ferric oxyhydroxides, *Geobiology*, 1: 169-178.

Anderson, J. R., Elzea, J., and Rich, F. J., 1999. Tertiary / Cretaceous Stratigraphy and Paleontology of the north central Coastal Plain of Georgia. Field Trip 8, *Southeastern Section of Geological Society of America.*

Clarke, J. S., Falls, W. F., Edwards, L. E., Frederiksen, N. O., Bybell, L. M., Gibson, T. G., and Litwin, R. J., 1994, Geologic, Hydrologic, and Water-quality data from a multi-aquifer system in coastal plain sediments near Millers Pond, Burke county, Georgia, 1992-93, *Georgia Geological Survey Information Circular* 96, 34 p.

Clarke, J. S., Falls, W. F., Edwards, L. E., Frederiksen, N. O., Bybell, L. M., Gibson, T. G., Gohn, G. S., and Fleming, F., 1996, Hydrogeologic data and aquifer interconnection in a multi-aquifer system in coastal plain sediments near Millhaven, Screven county, Georgia, 1991-95, *Georgia Geological Survey Information Circular* 99, 43 p.

Cooke, C. W., 1943, Geology of the Coastal Plain of Georgia, *U.S. Geological Survey Bulletin* 941, 121 p.

Cooke, C. W., and Shearer, H. K., 1918, Deposits of Claiborne and Jackson age in Georgia, *U.S. Geological Survey Professional Paper* 120, p. 41-81.

Dowling, D., Anderson, J. R, Wimberly, T., Amanambu, G., Gullet-Young, C., and Elliott, W. C., 2000, Sedimentology, clay mineralogy, and biostratigraphy of the Sandersville limestone in Georgia, *Southeastern section of the Geological Society of America abstracts with programs,* p. 32.

Dunham, R.J., 1962, Classification of carbonate rocks according to depositional texture, Mem. *American Association of Petroleum Geology* 1. p. 108-121.

Edwards, L. E., Frederikson, N. O., Bybell, L. M., Gibson, T. G., Gohn G. S., Bukry, D., Self-Trail, J. M., and Litwin, R. J., 2001, Overview of the Biostratigraphy and Paleoecology of sediments from five cores from Screven and Burke Counties, Georgia, IN Geology and Paleontology of Five Cores from Screven and Burke counties, Eastern Georgia, Ed. Edwards, L. E., *U.S. Geological Survey Professional Paper* 1603, 1603-B:B1-A19.

Falls, W. F., and Prowell, D. C, 2001, Stratigraphy and Depositional Environments of sediments from five cores from Screven and Burke Counties, Georgia, IN Geology and Paleontology of Five Cores from Screven and Burke counties, Eastern Georgia, Ed. Edwards, L. E., *U.S. Geological Survey Professional Paper* 1603, 1603-A:A1-A20.

Folk, R.L., 1962, Spectral subdivision of limestone types: *American Association of Petroleum Geologists Memoir.* 1, p. 62-84

Foote, J.; Elliott, E.; Rhedrick, K.; Williams, D.; Anderson, J.; Young, C.; and Elliott, W. C., 2003, Lithology and Paleontology of the Sandersville Limestone Member of the Tobacco Road Sandstone on the Coastal Plain of Georgia, *Southeastern Section of the Geological Society of America abstracts with programs,* 35(1):25.

Flugel, E., 1982, *Microfacies Analysis of Limestones*, New York: Springer-Verlag Berlin Heidelberg, 633 p.

Harris M.K., Thayer P.A., and Amidon M.B., 1997, Sedimentology and depositional environments of middle Eocene terrigenous-carbonate strata, southeastern Atlantic Coastal Plain, USA: *Sedimentary Geology*, 108:141-161.

Huddlestun, P. F, and Hetrick, J. H., 1978, Stratigraphy of the Tobacco Road Sand – a New Formation: in- Platt, P.A., (ed.), Short Contributions to the geology of Georgia; *Georgia Geological Survey Bulletin* 93, p. 56-77.

Huddlestun, P. F, and Hetrick, J. H, 1986, Upper Eocene Stratigraphy of Central and Eastern Georgia. Department of Natural Resources Environmental Protection Division *Georgia Geologic Survey, Bulletin* 95, p. 46-47.

Hurst, V. J., and Pickering, S. M., 1997, Origin and classification of coastal-plain kaolins, southeastern USA, and the role of groundwater and microbial action, *Clays and Clay Minerals*, 45:274-285.

Jackson, M.L.,1985, Soil Chemical Analysis—Advanced Course. 2nd Edition. 11th Printing. Published by the author. Madison, WI 895 p.

Kogel, J., Pickering, S.M., Jr., Shelobolina, E., Yuan, J., Chowns, T.M., and Avant, D.M., Jr., 2000, Geology of the Commercial Kaolin Mining District of Central and Eastern Georgia, *Georgia Geological Society Guidebook*, v. 20, No. 1, 3-17.

LaMoreaux, P. E., 1946a, Geology of the Coastal Plain of east-central Georgia, *Georgia Geological Survey Bulletin* 50, 26 p.

LaMoreaux, P. E., 1946b, Geology and groundwater resources of the Coastal Plain of east-central Georgia, *Georgia Geological Survey Bulletin* 52, 173 p.

Moore, D.M., and Reynolds, R.C., Jr., 1997. *X-Ray Diffraction and the identification and Analysis of Clay Minerals*: New York: Oxford University Press, 378 p.

Pajewski, K.A., Germano, J.M Tourscher, S.N., Anderson, J.R., Young, C.D., and Elliott, W.C., 2000. Micropaleontology, clay mineralogy and petrology of the Eocene Sandersville Limestone, Georgia, *Geological Society of America abstracts with programs* Annual meeting, 32(7):A-272.

Pierson, R. E., 1951, Possible Stratigraphic Relationships of the Sandersville Limestone to the Ocala Limestone of

West Georgia. Unpublished master's thesis from Emory University

Pickering, S. M, Jr., 1970, Stratigraphy, Paleontology, and Economic Geology of portions of Perry and Cochran Quadrangles, *Georgia, Georgia Geological Survey Bulletin* 81. 67 p.

Pickering, S. M., Hurst, V. J., and Elzea, J. M., 1997, Mineralogy, Stratigraphy, and Origin of Georgia Kaolins, *Field Excursion F4, 11th International Clay Conference*, Ottawa, Canada, 69 p.

Stephens, E. C., Gullett-Young, C., Elliott, W. C., Wampler, M., and Anderson, J. R., 2005, Glass and glaucony from the Ocmulgee Formation on the coastal plain of Georgia, age and origin, *Southeastern section of the Geological Society of America abstracts with programs*, 37(2):44.

Stephens, E. C., Anderson, Jr., J. R., Gullet-Young, C., Wampler, J. M., and Elliott, W. C., 2007, Age of the Ocmulgee Limestone (Georgia Coastal Plain) based on revised methodology for the K-Ar age of Glaucony, *Southeastern Geology* 45(1):15-24.

Suurmeyer, N., Howell, E., Powell, R., Smith, A., Anderson, J., Young, C., and Elliott, C., 2003, Microfacies correlation of the Upper Eocene Sandersville Limestone Member of the Tobacco Road Sand to the Ocmulgee Formation on the Coastal Plain of Georgia, *Geological Society of America abstracts with programs*, Annual Meeting 34(7):192.

Thiry, M., and Milnes, A. R., 1991, Pedogenic and groundwater silcretes at Stuart Creek Opal Field, South Australia. *Journal of Sedimentary Petrology*, 61(1):111-127.

Thiry M, and Ribet I., 1999 Groundwater silicification in Paris basin limestones: fabrics,

mechanisms and modeling. *Journal of Sedimentary Research* 69:171– 183.

Tucker, M.E., and Wright, V.P., 1990, *Carbonate Sedimentology*: London, Blackwell Scientific Publications, 482 pp.

Veatch, J.O., and Stephenson, L. W., 1911, Preliminary report on the geology of the Coastal Plain of Georgia, *Georgia Geological Survey Bulletin* 26, 466 p.

Wortman, S., Stephens, E., Lawrie, K., Burger, E., Gullett-Young, C., Foote, J., Anderson, J., and Elliott, C., 2004, Correlation of Upper Three Runs Aquifer to the Eocene Sandersville Limestone Coastal Plain, Georgia, *Geological Society of America abstracts with programs*, Annual Meeting, 36(5):80.

Young, C., Anderson, J., and Elliott, W. C., 2003, The Sandersville Limestone Member of the Tobacco Road Sandston (Eocene), Coastal Plain of Georgia, *Southeastern Section of the Geological Society of America abstracts with programs,* 35(1):54

SOUTHEASTERN GEOLOGY
V. 47, No.4, November 2010, p. 207-217

A NEW SPECIES OF *ABERTELLA* (ECHINOIDEA, SCUTELLINA) FROM THE LATE MIOCENE (TORTONIAN) PEACE RIVER FORMATION OF HARDEE COUNTY, FLORIDA

[1]ADAM S. OSBORN AND CHARLES N. CIAMPAGLIO[2]

[1]1500 Lakeshore Drive, Camden, SC 29020, Macropneustes@Netzero.com
[2] Earth and Environmental Sciences, Wright State University – Lake Campus, 7600 Lake Campus Drive, Celina, OH 45822

ABSTRACT

A new species of clypeasterid echinoid, *Abertella dengleri* n. sp., from the late Miocene Peace River Formation, Hardee County, Florida is described and discussed. Specimens of *Abertella dengleri* n. sp., have been recorded in the literature as *Abertella aberti* (Conrad 1842); however, this paper will demonstrate that these specimens represent a distinct species, with a latitudinally elongate test that is consistent and distinct and readily distinguishes it from the subcircular test of *Abertella aberti* (Conrad 1842) of the middle Miocene of the east coast of North America. The elongate test of *A. dengleri* n. sp., also distinguishes it from all other described species of *Abertella*. This new large species of sand dollar has remained virtually anonymous in the bed of the Peace River, one of America's most popular fossil collecting locations, in a very urban area near Zolfo Springs, Hardee County Florida. *Abertella dengleri* n. sp., now joins *Abertella aberti* (Conrad 1842) as the second North American species of the genus *Abertella,* and with a late Miocene age, it is the youngest of the two.

INTRODUCTION

Abertella dengleri n. sp., occur in a dense accumulation of largely fragmented, agatized, specimens, in a horizon of sandy, siliclastic dolostone less than 20 cm in thickness, within the late Miocene Peace River Formation. The locality occurs in the bed of the Peace River three kilometers upriver from Zolfo Springs, Hardee County Florida (Figure 1). The *Abertella* bed is largely devoid of other invertebrates, with the exception of rare specimens of the echinoids *Rhyncholampas* aff. *chipolanas* (Oyen and Portell 1996), a large undescribed *Brissopsis* that reaches a length in excess of 90 mm (currently being studied by the authors), and spines of an undetermined cidarid, similar to *Prionocidaris cookei* (Cutress 1976). The restricted horizon in which *Abertella dengleri* n. sp., occurs contains a profusion of *Abertella* fragments, although complete specimens are rare. Specimens that are collected are often corroded, abraded and chipped as they weather free from the very resistant, chert-rich matrix in the river bed, typically rendering the surface details of the specimens indiscriminant and obscure.

Specimens of *Abertella* from this region of Florida have been discussed in the literature as *Abertella aberti* (Conrad 1842) (Mckinney 1985, Oyen 2001); but, closer examination reveals that these specimens belong to a distinct species, with a latitudinally elongate test, (Table 1 and Figure 2) shallow or absent indentations opposite the anterior ambulacra, and a pronounced and narrow posterior notch that distinguishes it from the subcircular test of *Abertella aberti* (Conrad 1842) (Table 2 and Figure 3) and all other described members of the genus (Figure 4).

OVERVIEW OF THE GENUS

The genus *Abertella* is restricted to the Miocene Epoch, and is found along the east coast of the Americas from Argentina to Maryland (Martinez, et al., 2005). The genus ranges to the end of the Miocene, apparently being displaced by northward migrating mellitid sand dollars (Smith 1984).

With the addition of *Abertella dengleri* n. sp.,

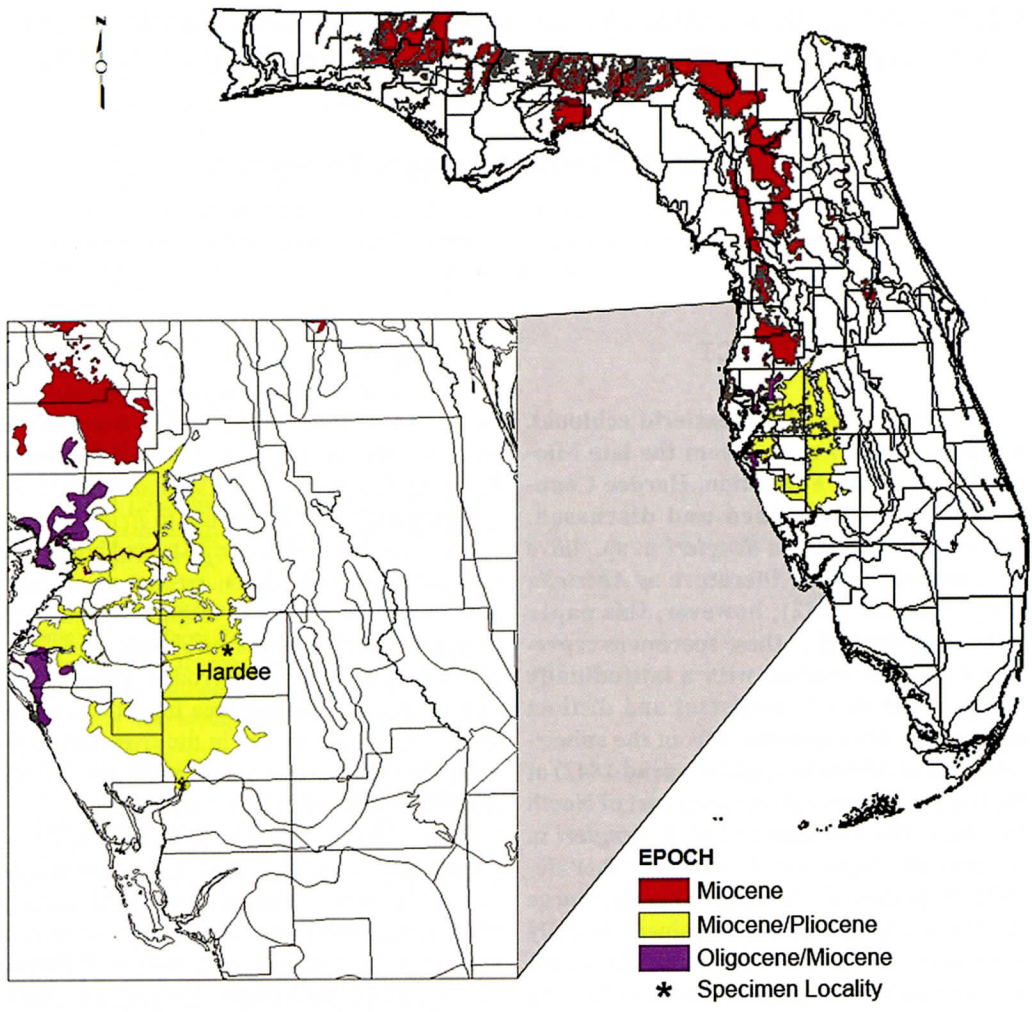

Figure 1: Outcrop zone of Pliocene-Oligocene strata in Florida. Hardee County collecting area is noted.

the genus *Abertella* Durham now contains eight species (Figure 4): *A. aberti* (Conrad 1842), *A. cazonensis* (Kew 1917), *A. gualichensis* (Martinez, et al., 2005), *A. habensis* (Sanchez Roig 1949), *A. kewi* (Durham 1957), *A. palmeri* (Durham 1957), *A pirabensis* (Marchesini Santos 1958) and the species described herein: *A. dengleri* n. sp., (Durham 1953; 1955; 1957; Martinez and Mooi 1997; Martinez, et al., 2005; Mooi 1989). *Abertella dengleri* n. sp., is now the second species of *Abertella* described from North America.

Durham (1953) named the genus *Abertella*, to differentiate it from *Scutella.* He choose Scutella *aberti* (Conrad 1842) from the middle Miocene age Choptank Formation of Maryland as the type species of the genus. *A. aberti* remained the only described *Abertella* from North America until one hundred years later when Cooke (1942) described *Scutella floridana* from Miocene strata of the Chipola Formation near Sopchoppy, Wakulla County, Florida. Durham (1953) suggested that *Scutella floridana* (Cooke 1942) should be placed in the new genus *Abertella*; however, Cooke (1959), the original author, later synonymized his own *Scutella floridana* with *Abertella aberti* (Conrad 1842), leaving *Abertella aberti* (Conrad 1842) once again as the only described member of the genus from North America. *Abertella aberti*

Table 1. Measurements of Abertella dengleri n, sp. Empty fields are indeterminable due to test preservation or incompleteness, All measurements are in millimeters. *denotes specimens plotted in figure 1. Non-type specimens reside in private collections. (am=ambulacrum)

Specimen	Width	Length	Height	W to L ratio	Amb 1	Amb 2	Amb 3	Amb 4	Amb 5	Periproct Width	Peristome Width
NCSM11393	*144	104		1.38							
	*139	97		1.43							
	*125	96	10	1.30						4	
	*117	85		1.37	31	31	28	31	31		
	*118	85		1.38	25	25	22	25	25	4.5	
	*111	82		1.35							
	*71	56		1.26							
	*54	41		1.31							
	*47	31		1.51							
	*36	26		1.38							
NCSM11396		82			27	27		27	27		
		81			25	25	22	25	25		3
					26	26		26	26		
NCSM11394		77	9		26	26	23		26	3.5	
			11		30		26		30		
					29	29	26.5	29	29		

(Conrad 1842), which was initially described from the Middle Miocene Choptank Formation of Maryland, is now known to have a much broader geographical range, and also occurs in the middle Miocene Pungo River Marl of North Carolina (Kier 1983) and the Middle Miocene Chipola Formation and Hawthorn Group of Florida (Clark 1904; Clark and Twitchell 1915; Cooke 1959; Williams, et al., 1977).

In describing the genus *Abertella*, Durham (1953) moved *Scutella cazonensis* (Kew 1917), from the Miocene of Mexico, and *Scutella habanensis* (Sanchez Roig 1949), from the Miocene(?) of Cuba, to the new genus. He postulated that further study would be required to determine if *Echinarachnius sebastiana* (Jackson 1922) from the Oligocene(?) of Puerto Rico should be placed within the genus. Four years later, Durham (1957) described and named *Abertella palmeri*, from the early Miocene of Guatemala, and *Abertella kewi*, from the middle Miocene of Chiapas, Mexico.

Brito (1981) described and named *Abertella complanata* from the Miocene of Brazil, though Martinez and Mooi (1997) stated that this species is synonymous with *Karlaster pirabensis* (Marchesini Santos, 1958), a previously described species from the same beds, and that they should both belong to a single species that should take the name *Abertella pirabensis* (Marchesini Santos 1958) (Martinez, et. al., 2005).

Abertella gualichensis (Martinez, et al., 2005) from the early-mid Miocene of Argentina, is the most recent species to be described in the genus, and is the southernmost member of the genus.

GEOLOGIC SETTING

Abertella dengleri n. sp., specimens described herein were collected from the late Miocene (Tortonian) age, lower unit of the Peace River Formation, found within the bed of the Peace River, three kilometers upriver from Zolfo Springs, Hardee County, Florida (Figure 1) (Scott and Campbell 1993).

In the area of study, the Hawthorn Group generally consists of a basal carbonate unit, the Arcadia Formation, and an upper siliclastic

Table 2: Measurements of *Abertella aberti* (Conrad 1842) specimens plotted in figure two, from the Middle Miocene Choptank Formation, Scientists Cliffs, MD. Empty fields are indeterminable due to test preservation or incompleteness. All measurements are in millimeters. (amb=ambulacrum)

Width	Length	W to L ratio	Amb 1	Amb 2	Amb 3	Amb 4	Amb 5
17	17	1.00					
19	18	1.05					
34	32	1.06					
37	37	1.00					
46	43	1.06					
52	51	1.01					
53	54	.98					
69	69	1.00					
76	74	1.02					
79	78	1.01					
81	78	1.03	25	22	22	22	25
89	84	1.05					
92	90	1.02					
99	96	1.03					
99	96	1.03	32	29	29	29	32
109	110	.99	35	32	32	32	35
110	110	1.0	36	33	33	33	36
116	110	1.05					
119	114	1.04	39	36	36	36	39
121	121	1.0					
132	128	1.03					

unit, the Peace River Formation (Scott, 2001). The Hawthorn Group has been problematic since it was named by Dall and Harris (1892). It is a complex unit of interbedded and intermixed carbonate and siliclastic sediments containing varying concentrations of phosphate (Scott 1990). Scott (1988) upgraded the Hawthorn to group status in Florida and defined its component formations (Figure 5).

The Peace River Formation is exposed beneath a thin layer of overburden, on the southern part of the Ocala Platform, extending into the Okeechobee Basin in south Florida (Scott 2001). The unit reaches a maximum known thickness of 650ft (198m) in the Okeechobee basin (Scott, 1990), and is unconformably underlain by the late Oligocene to middle Miocene Arcadia Formation, which is largely a subsurface unit throughout it's extent (Scott 1988). The Peace River Formation is typically overlain by the early Pliocene Tamiami Formation (Missimer 2002). Missimer (2002) divided the Peace River Formation into distinct lower and upper stratigraphic units. The lower unit is late Miocene (Tortonian), and consists of relatively flat-bedded, predominantly siliclastic, nearshore ramp, beach and carbonaceous lagoonal deposits, and is capped by a distinct disconformity. The upper unit is a mixed siliclastic/carbonate unit containing deltaic characteristics, such as graded beds and angular bedding, of early Pliocene (Zanclean) age (Missimer, 2002).

The siliclastics of the Peace River Formation are typically dolomitic, phosphatic, clayey quartz sands. Carbonate beds are common and are generally sandy, phosphatic, clayey dolostones (Scott, 1990), however, the siliclastic

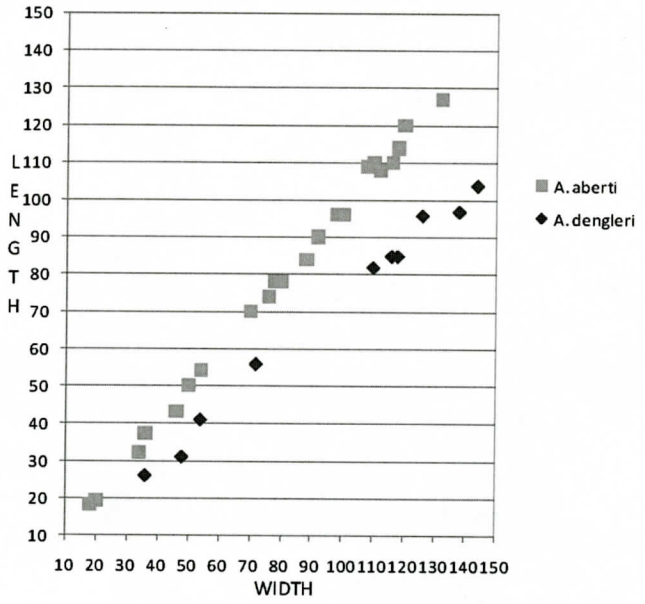

Figure 2. Chart displaying comparison of length to width ratios of *Abertella aberti* (Conrad 1842) and *Abertella dengleri* n. sp. Sample made with 15 specimens of *Abertella aberti* (Conrad 1842) from the Choptank Formation of Scientists Cliffs Maryland, and 10 specimens of *Abertella dengleri* n. sp., from the Peace River Formation, Hardee County, Florida. All measurements are in millimeters.

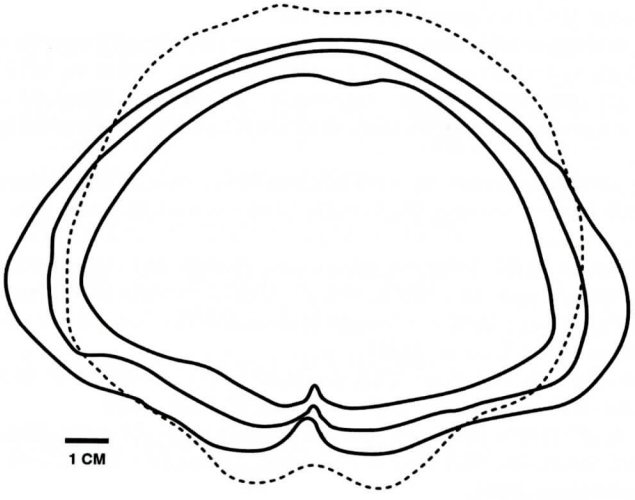

Figure 3: Marginal outlines of three specimens of *Abertella dengleri* n. sp., and a specimen of *Abertella aberti* (stippled) for comparison.

component predominates and is the distinguishing lithologic feature of the unit. The siliclastics typically comprise two-thirds or more of the Peace River Formation (Scott, 1988). Strontium-isotope data enabled Missimer (2002) to provide an age range of 11 to 8.5 Ma for the lower Peace River Formation, and 5.23 to 4.29 Ma for the upper unit.

Lithologic units of the phosphate-rich Hawthorn Group are characterized as being deposited in inner shelf, nearshore environments. During the early Miocene, terrigenous siliclastics derived from the southern Appalachians filled the Gulf Trough, and encroached into the

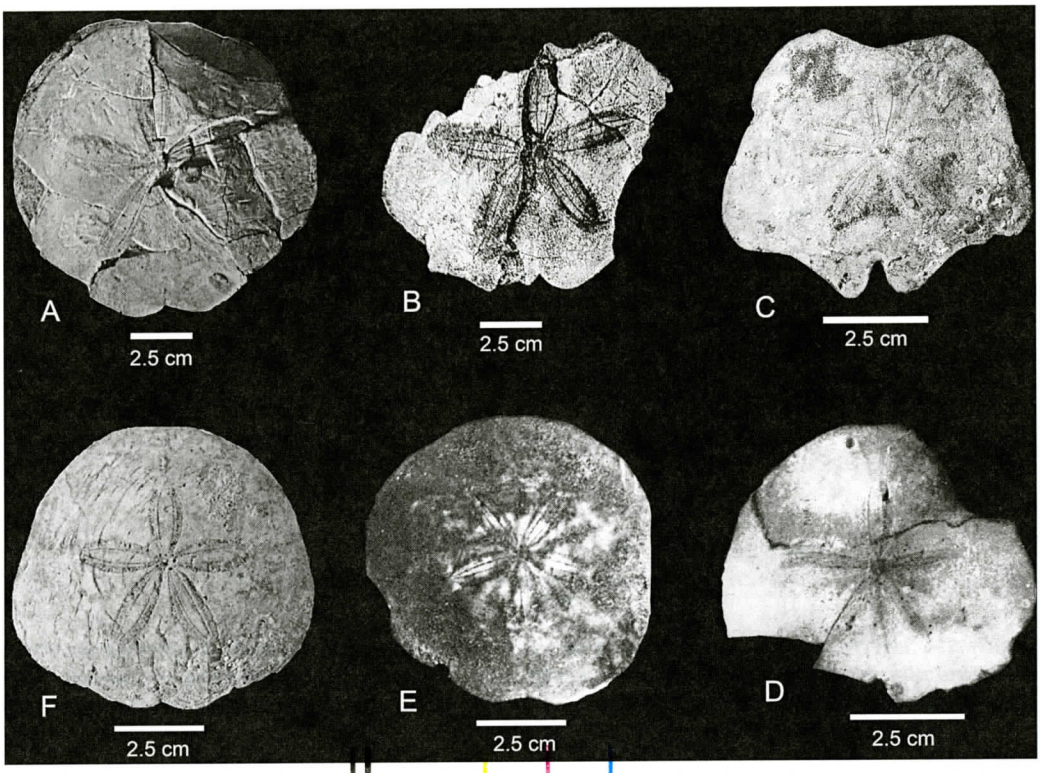

Figure 4: Type specimens of species of the genus *Abertella* (*Abertella dengleri* n. sp., is figured in Figure 6, and *Abertella aberti* (Conrad 1842) is figured in Figure 7.)
A: *Abertella cazonensis* (Kew 1917), holotype, Cal Academy of Science #369, aboral view; Near Cazones River, Papantla Region of Mexico. W111mm x L105mm (From Dickerson and Kew, 1917.)
B: *Abertella kewi* (Durham 1957), most complete paratype, University of California Museum of Paleontology #36497, aboral view; Simojovel, Chiapas Mexico. W92mm x L88mm—estimated by Durham. (From Durham, 1957.)
C: *Abertella palmeri* (Durham 1957), paratype, University of California Museum of Paleontology #36504; aboral view; Rio Salinas, West Peten Province, Guatemala. W68.9mm x L60.5mm. (From Durham, 1957.)
D: *Abertella pirabensis* (Marchesini Santos 1958), holotype, #4493 do Catalogo de Invertebrados de colecao da Divisao de Geologia e Mineralogia do D.N.P.M, Rio de Janerio; aboral view; Ponta de Pirabas, ilha Fortaleza, Esta do do Para Brazil. W66mm, length of incomplete holotype not provided by Marchesini Santos. (From Marchesini Santos, 1958)
E: *Abertella habanensis* (Sanchez Roig 1949), holotype, Call. Sanchez Roig; aboral view; Canteras de Arroyo Naranjo, Habana Cuba. W73mm x L69mm. (From Sanchez Roig, 1949.
F: *Abertella gualichensis* (Martinez, et al., 2005), Holotype, Museo Argentina de Ciencias Naturales #4714; aboral view; Salina del Gualicho, Rio Negro Province, Argentina. W84.3mm x L77.6mm. (From Martinez, Reichler and Mooi, 2005)

carbonate producing environments of peninsular Florida. These siliclastics represent the first recorded Cenozoic influx of terrigenous sediments onto the carbonate bank of peninsular Florida (Scott, 1990). This change from carbonate to siliclastic deposition was, in part, due to the continued influx of large amounts of siliclastics from the southern Appalachians (Scott 1988).

The *Abertella* biozone occurs within the lower Peace River Formation, in light gray, weathered brown, siliclastic dolostone that is rich in opaline chert. The strata represents a terrigenous marine facies, where near shore habitats were subject to significant inputs of coarse clastic material from a prograding Miocene delta

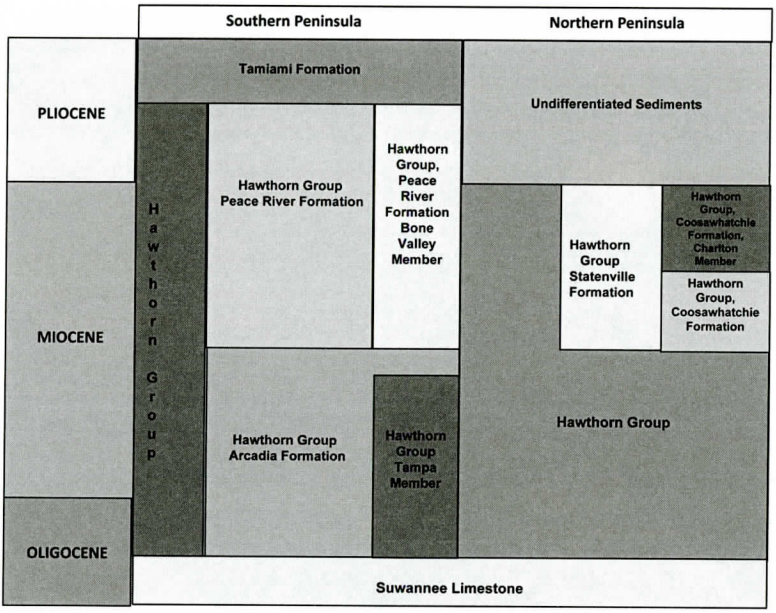

Figure 5: Generalized stratigraphic column for the Miocene of Peninsular Florida, (from Scott 2001).

(McKinney 1985). Though molluscs are not uncommon in the horizons above and below the *Abertella* biozone, they are rare within it.

SYSTEMATIC PALEONTOLOGY

Figured specimens of *Abertella dengleri* n. sp. are housed at the North Carolina Museum of Natural Sciences (NCSM) in Raleigh.

Class ECHINOIDEA Leske, 1778

Order CLYPEASTEROIDA A. Aggassiz, 1872

Suborder SCUTELLINA Haeckel, 1896

Family ABERTELLIDAE Durham, 1955

Type genus *Abertella* Durham, 1953

Type species *Scutella aberti* (Conrad, 1842) by original designation

Abertella dengleri, new species (Figure 6)

Diagnosis: *Abertella* in which the test is large, thin, and significantly more laterally elongate than other members of the genus. The nearly elliptical anterior margin typically lacks indentations opposite the anterior ambulacra, when present they are faint and shallow. Ambulacrum III is typically 90% the length of the other ambulacral, and the posterior notch is pronounced and narrow.

Description: Test thin, large, marginal outline laterally elongate: test much wider than long (Table 1). Upper surface slightly domed in the apical region, flat marginally. Margin thin with marginal indentations opposite ambulacra I and V, with a very well developed, narrow, posterior notch; anterior margin gently rounded, often nearly elliptical, indentations opposite anterior ambulacra faint and shallow, when present. Oral surface flat, surface covered with abundant fine tubercles. Apical system fused, central, slightly elevated, hydropores numerous on star-shaped madreporic plate which extends between the ambulacra; four genital pores at terminus on suture between madreporic plate and first plates of the interambulacra column. Ambulacra lanceolate, extending 60-70% of the radius, slightly open, truncated at tips, ambula-

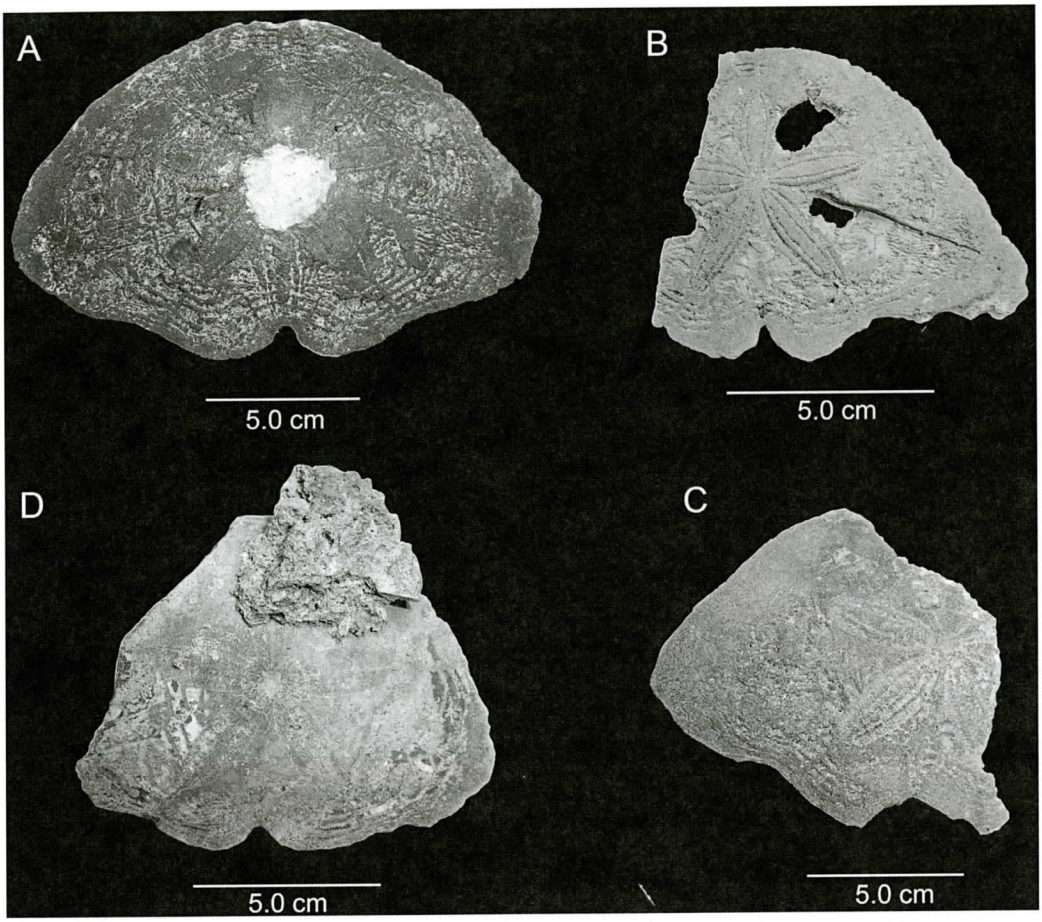

Figure 6: Type Specimens of *Abertella dengleri* n. sp. Type specimens are housed at the North Carolina Museum of Natural Science.
A: *Abertella dengleri* n. sp., holotype, NCSM11393: aboral view, Peace River Formation, Hardee County, Florida (W144mm x L104mm)
B: *Abertella dengleri* n. sp., paratype, NCSM11394: aboral view, Peace River Formation, Hardee County, Florida (W82mm x 77mm)
C: *Abertella dengleri* n. sp., paratype, NCSM11395: aboral view, Peace River Formation, Hardee County, Florida (W89mm x L75mm)
D: *Abertella dengleri* n. sp., paratype, NCSM11396: aboral view, Peace River Formation, Hardee County, Florida (W103mm x L82mm)

crum III slightly shorter, typically 90% the length of the paired ambulacra; pores small, circular, deeply conjugate, inner row nearly straight, outer row slightly arched. Ambulacra narrow in petaloid region, expanding considerably beyond the petals where they are considerably wider than interambulacral areas. Interambulacra narrowing from outer ends of the petals to the margin. Oral surface flat, food grooves strongly developed, bifurcating close to peristome with numerous secondary branches near the margin. Peristome central, small, circular. Periproct smaller than peristome, circular, submarginal, close to base of posterior notch. Interambulacra on oral face interrupted by basicornal ambulacral plates.

Discussion: *Abertella dengleri* n. sp., is readily differentiated from its geographically nearest congener, *Abertella aberti* (Conrad 1842), and all other described species of *Aber-*

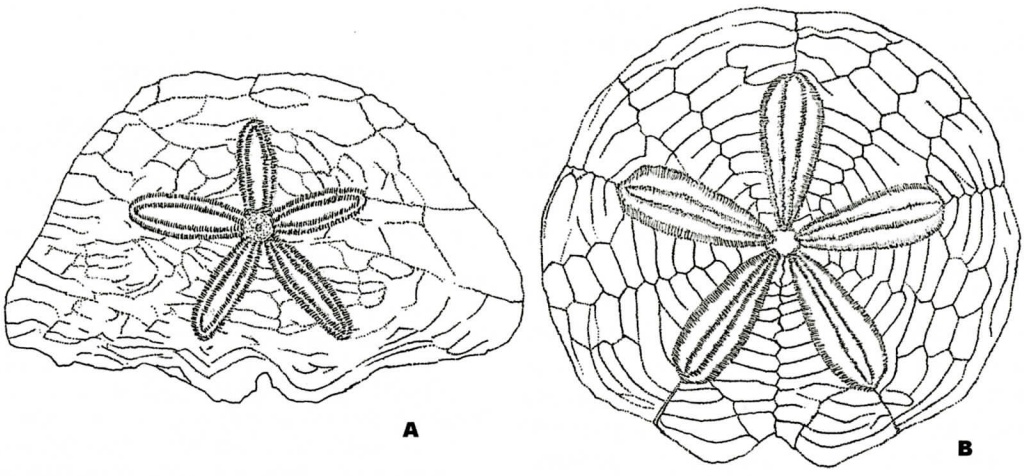

Figure 7: Camera lucida comparison of A: *Abertella dengleri* n. sp., a composite made from three specimens, Peace River Formation, Hardee County Florida and B: *Abertella aberti* (Conrad 1842) from the Middle Miocene Choptank Formation, Scientists Cliffs, MD.

tella, by its greatly elongate test (Figure 7). The average width to length ratio of ten measured specimens of *Abertella dengleri* n. sp., is 1.37 (Table 1 and Figure 2), whereas the average width to length ratio of twenty-one measured specimens of *Abertella aberti* (Table 2) is 1.03. Additional traits that distinguish *Abertella dengleri* n. sp., from *Abertella aberti* (Conrad 1842) include the narrower posterior notch, and the tendency for ambulacrum III to be merely 88-91% of the length of the paired ambulacra (Table 1). Conversely, ambulacrum III is typically the same length as ambulacra II and IV in *Abertella aberti* (Conrad 1842), with ambulacra I and V being 10% longer than the other ambulacra in *Abertella aberti* (Table 2). Furthermore, the margin of *Abertella dengleri* n. sp., does not typically contain the broad shallow indentations opposite each of the three anterior ambulacra that are consistently present in the test of *Abertella aberti* (Conrad 1842). When present, the indentations are faint and largely undiscernable. The anterior margin of the test is often nearly elliptical in appearance. The corroded surface of the tests available for study prohibit close study of the oral surface, so finer differences and similarities between the oral surfaces of *Abertella dengleri* n. sp., and *Abertella aberti* (Conrad 1842) could not be determined.

Though other morphological factors serve to separate *Abertella dengleri* from all other described species of *Abertella*, the marginal outline and W/L ratio, which gives the test a very elongate appearance, is the most obvious factor that readily differentiates it from its congeners. The holotype of *Abertella palmeri* (Durham 1957) has a width to length ratio of 1.13, and though this species does have wing-like lateral extensions which give it a greater width to length ratio than other previously described species of *Abertella*, the test retains a considerable length compared to it's width in comparison with *Abertella dengleri* n. sp. The test of *Abertella palmeri* (Durham 1957) also has a roughly pentagonal outline, versus the nearly elliptical anterior margin of *Abertella dengleri.* Durham's (1957) estimated measurements for the holotype of *Abertella kewi* (Durham 1957) give it a W/L ratio of 1.05. Furthermore, the test of *Abertella kewi* (Durham 1957) has a subcircular outline, with greater anterior marginal indentations than *Abertella dengleri.* The holotype of *Abertella habanensis* (Sanchez Roig 1949) has a W/L ratio of 1.05 and is subcircular in outline, and *Abertella cazonensis* (Kew 1917) has a W/L ratio of 1.05 and is also subcircular in outline which readily differentiates it from *Abertella dengleri* n.sp. The holotype of *Echinarachnius* (possibly *Abertella*) *sebastiana* (Jackson 1922) has a W/L ratio of

1.12. *Abertella pirabensis* (Marchesini Santos 1958) is subcircular in outline and the holotype of *Abertella gualichensis* (Martinez, et al., 2005) has a W/L ratio of 1.08. Furthermore, *Abertella guulichensis* (Martinez, et al., 2005) has a much less pronounced, shallower and wider posterior anal notch, and a nearly circular marginal outline which clearly differentiates it from *Abertella dengleri* n. sp.

Material: Holotype NCSM11393 (Figure6A). Paratypes: NCSM11394 (Figure 6B), NCSM11395 (Figure 6C) and NCSM11395 (Figure 6D). Material examined includes the holotype, three paratypes and twelve less complete, non-paratype specimens collected by the first author and Fred Dengler from the Peace River, one to three kilometers upriver from Zolfo Springs, Hardee County, Florida.

Measurements: Measurements for all examined specimens are given in table 1.

Etymology. This species is named in honor of Fred Dengler of Bartow, Florida.

Occurrence. *Abertella dengleri* n. sp., has not been definitively identified outside of Hardee County, Florida where it occurs in the late Miocene age lower unit of the Peace River Formation in the bed of the Peace River near Zolfo Springs.

ACKNOWLEDGEMENTS

We thank Fred Dengler of Bartow, Florida for his specimen contributions and guiding the first author on numerous trips up river collecting this echinoid. Without his dedication and generosity, and "seeing beyond the vertebrate fossils", this species would remain undescribed. We also thank Mike Ellwood, of Scientists Cliffs, Maryland for providing specimens of *Abertella aberti* (Conrad 1842), and guiding the first author on numerous collecting trips to the richly fossiliferous Scientist Cliffs of Maryland to collect specimens of *Abertella aberti* (Conrad 1842) for comparison purposes. We are also indebted to David Bohaska for providing specimens of *Abertella aberti* (Conrad 1842) for measurements, and Andrea Ciampaglio, whose illustrations were vital to the completion of this paper.

REFERENCES CITED

Aggassiz, A. 1872. Revision of the Echini. Memoirs of the Museum of Comparative Zoology, Harvard, 3:1-762

Brito, I.M. 1981. *Contribuição à Paleontologia do Estado do Pará. A ocorrência de Abertella (Echinoidea, Clypeasteroidea) na* Formação *Pirabas* Boletim do Museu Paraense Emilio Goeldi, n.s., Geologia 23: p. 1-8

Clark, Bullock, WM. 1904. Echinodermata, in: Maryland Geological Survey Miocene, p. 430-433.

Clark, W.R., and Twitchell, M.W. 1915. The Mesozoic and Cenozoic Echinodermata of the United States. United States Geological Survey Monograph 54, 341 p.

Conrad, T.A. 1842. Observations on a portion of the Atlantic Tertiary region, with a description of a new species of organic remains. Proceedings of the National Institute for the Promotion of Science, 2: p.171-194.

Cooke, C.W. 1942. Cenozoic irregular echinoids of the eastern United States, Journal of Paleontology, 16 (1), p. 1-62.

Cooke, C.W. 1959. Cenozoic echinoids of eastern United States: U.S. Geological Survey Professional Paper, v. 321, p 1-106, p. 1-43.

Cutress, B.M. 1976. A new *Prionocidaris* (Echinodermata; Echinoidea) from the Middle Miocene of Florida. Biological Society Washington, Proceedings, Vol. 89, p. 191-198, Fig. 1-2.

Dall, W.H. and Harris, G.D. 1892, Correlation paper-Neocene. United States Geological Survey Bulletin #84, p 85-158.

Kew in, Dickerson, R.E., and Kew. W.S.W. 1917. The fauna of a medial Tertiary Formation and the associated horizons of northeastern Mexico. Proceedings of the California Academy of Sciences, Series 4, 7: p. 125-156.

Durham, J.W. 1953. Type species of *Scutella*. Journal of Paleontology, 27: p. 347-352.

Durham, J.W. 1955. Classification of clypeasteroid echinoids. University of California Publications in Geological Sciences, 31: p. 73-198.

Durham, J.W. 1957. Notes on echinoids. Journal of Paleontology, 31: p. 625-631.

Haeckel, E.H.P.A 1896. Systematische Phylogenie. Entwurf eines Natuerlichen Systems der Organismen auf Grund ihrer Stammesgeschichte. Zweiter Theil: Systematische Phylogenie der Wirbellosen Thiere (Invertebrata), Berlin, 720p.

Jackson, R.T. 1922. Fossil Echini of the West Indies. Publications of the Carnegie Institution of Washington, 306: p. 1-104.

Kier, P.M. 1983. Upper Cenozoic echinoids from the Lee Creek mine, in: Geology and paleontology of the Lee Creek mine, North Carolina, I. Smithsonian Contributions to Paleobiology, No. 53: p. 499-507.

Leske, N. G. 1778, Additamenta ad Jacobi Theodori Klein naturalem dispositionem Echinodermatum et lucubratiunculam de aculeis echinorum marinorum. Lipsiae,

Lepzig, 278p.

Marchesini Santos, M.E. 1958. *Equinóides Miocénicos da Formação Pirabas. Departamento Nacional* da *Produção Mineral, Divisão de Geologia e Mineralogia*, Boletim, 179: p. 1-24.

Martinez, S. and R. Mooi. 1997. *"Karlaster" pirabensis* from the Brazilian Miocene is a species of *Abertella* (Scutellina, Echinoidea), not a monophorasterid. 15 Congresso Brasileiro de Paleontologia, Sao Paulo, 61p.

Martinez, S., Reichler, V., and Mooi, R. 2005. A new species of *Abertella* (Echinoidea, Scutellina) from the Gran Bajo Del Gualicho Formation (Late Early Miocene-Early Middle Miocene), Rio Negro Province, Argentina, Journal of Paleontology, 79(6): p. 1229-1233.

Mckinney, M.L. 1985. The abundant occurrence of the middle Miocene sand dollar *Abertella aberti* in the Hawthorn Formation of Florida. Southeastern Geology, 25: p. 155-158.

Missimer, T.M. 2002. Late Oligocene to Pliocene evolution of the central portion of the South Florida platform: mixing of siliclastic and carbonate sediments. Florida Geological Survey Bulletin No. 65, 184p

Mooi, R. 1989. Living and fossil genera of the Clypeasteroidea (Echinoidea: Echinodermata); an illustrated key and annotated checklist. Smithsonian Contributions to Zoology, 488: p. 1-51.

Oyen, C.W. 2001. Biostratigraphy and diversity patterns of Cenozoic echinoderms from Florida, unpublished doctoral thesis, University of Florida, 438 p.

Oyen, C.W. and Portell, R.W., 1996. A new species of *Rhyncholampas* (Echinoidea: Cassidulidae) from the Chipola Formation: the first confirmed member of the genus from the Miocene of the southeastern U.S.A and the Caribbean. Tulane Studies in Geology and Paleontology, 29: p. 59-66.

Sanchez Roig, M. 1949. Paleontologia Cubana I, Los equinodermos fosiles de Cuba. Compania Editora de Libros y Foiletos, La Habana, 331p.

Scott. T.M. 1988. The lithostratigraphy of the Hawthorn Group (Miocene) of Florida. Florida Geological Survey, Bulletin No. 59, 148p.

Scott. T.M. 1990. The lithostratigraphy of the Hawthorn Group of peninsular Florida. Florida Geological Survey. Open file Report No. 36, p. 325-336.

Scott, T.M. 2001, Text to accompany the geological map of Florida. Florida Geological Survey, Open file report No. 80, 27p.

Scott. T.M. and Campbell, K. 1993. Geological Map of Hardee County, Florida. Florida Geological Survey, Open File Map Series No. 31

Smith. A.B. 1984. Echinoid Palaeobiology. George Allen and Unwin, London, 190p.

Williams, K.E., Nichol, D, and Randazzio, A.F. 1977. The geology of the western part of Alchua County. Florida Bureau of Geology, Report of Investigations No. 85: 54p.

SOUTHEASTERN GEOLOGY
V. 47, No.4, November 2010, p. 219-226

GROUNDERWATER-DEVELOPED FERRICRETES IN THE UPDIP CLASTIC LITHOFACIES OF THE CLAYTON FORMATION (LOWER PALEOCENE) ACROSS THE COASTAL PLAIN OF WEST-CENTRAL GEORGIA (USA)

CARL R. FROEDE JR.

U.S. Environmental Protection Agency
Region 4
61 Forsyth Street
Atlanta, GA 30303-8960

ABSTRACT

Ferricretes composed of ferrihydrite, goethite, limonite, and hematite minerals, are found in the updip clastic lithofacies of the Clayton Formation (lower Paleocene) on the Coastal Plain of west-central Georgia (USA). These iron-cemented layers have previously been attributed to the dissolution of the calcium carbonate facies of the Clayton Formation. Pedologists commonly attribute ferricretes to highly weathered soils in tropical to semi-tropical settings. However, recent work on the origin of ferricretes suggests that changes in groundwater geochemistry can also contribute to their formation and development. The ferricretes found in the Clayton Formation clastic lithofacies have not been created from the dissolution of limestone or from top down soil-forming processes. Rather, these iron-cemented layers have formed and developed from the oxidation of anaerobic ferrous groundwater within the shallow subsurface. The resulting ferricrete morphology is a result of the interplay between subsurface sedimentary and structural features and a dynamic groundwater table.

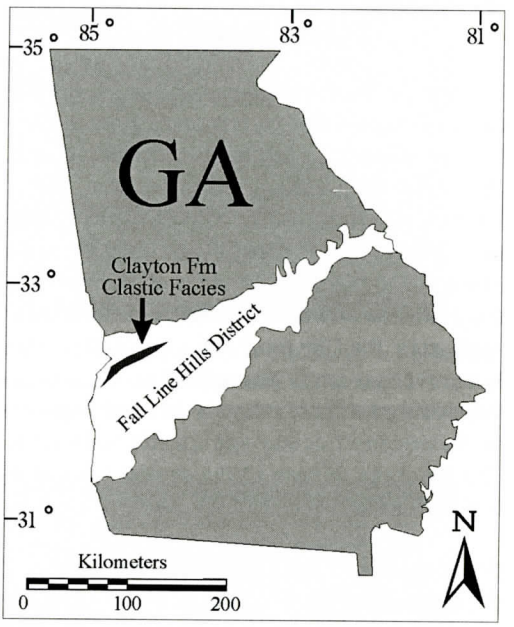

Figure 1. Generalized outcrop map of the updip clastic lithofacies portion of the Clayton Formation in the Fall Line Hills District across west-central Georgia. Ferricretes occur in many places in the subsurface and they vary in their morphology based on the interplay between changing oxidization conditions within the vadose zone and sedimentary and structural features. Modified from Alhadeff and others, 2001.

INTRODUCTION

Ferricretes composed of ferrihydrite, goethite, limonite and hematite minerals, are found in the updip clastic lithofacies of the Clayton Formation (lower Paleocene) on the Coastal Plain of west-central Georgia (USA) [Figure 1]. These iron-cemented layers have historically been interpreted as having been derived from the dissolution of the Clayton limestone (e.g., Veatch and Stephenson, 1911; Cooke, 1943; Eargle, 1955; Donovan, 1986; Reinhardt and others, 1994; Cocker, 2006). Only recently has the updip marine clastic lithofacies been recognized (Gibson, 1980, 1992;

Froede, 2008) and this interpretation requires the development of ferricretes from either pedogenic or hydrogeologic processes. The lack of any developed pedogenic soil horizons commonly associated with ferricretes suggests an origin from the oxidation of anaerobic ferrous groundwater. Their highly varied morphology is due to the interplay between subsurface sedimentary and structural features and a dynamic groundwater table.

IS THERE A PEDOGENIC SOURCE FOR THE IRON?

The Clayton Formation varies in its lithofacies as a function of its position across the former continental shelf (Reinhardt and Gibson, 1981; Gibson, 1982, 1992; Donovan, 1986; Froede and Reed, 2007; Froede, 2008). The stratigraphic unit is generally defined by updip nearshore marine clastic sediments and downdip middle to outer shelf carbonates. Within the study area, the Clayton Formation clastic lithofacies is consistently above the Late Cretaceous Providence Formation and is covered in places by Paleocene/Eocene-age clastic sediments. The lithology of each of the stratigraphic units is described as:

Paleocene/Eocene Clastic Sediments (Unnamed unit)

> The Clayton Formation clastic sediments within the study area are covered in places by reworked unnamed clastic sediments derived from updip exposures of the Clayton Formation. These generally orange to dark-orange-red clayey sand sediments are in places highly contorted and include ferricrete rip-up clasts of varying sizes—some resembling plinthite nodules (Froede, 2008, 2010).

Paleocene Clayton Formation (Updip clastic lithofacies)

> The most conspicuous constituent of the Clayton formation (sic) at the weathered outcrop is tough brick-red or maroon clayey sand, which contrasts strikingly with the light-colored unconsolidated Cretaceous sand and clay that underlie it. ... At many places the base of the formation is marked by an accumulation of brown iron ore (Cooke, 1943, p. 41).

Late Cretaceous Providence Formation

> The formation consists chiefly of white or light-colored generally crossbedded micaceous sand and lenses of white or light-colored massive clay (Cooke, 1943, p. 35).

As a marine clastic unit, the Clayton Formation would not likely have contained iron in an oxidized state within its original sediments. The ferric oxide would have developed during and/or following sea level withdrawal with the oxidation of the stratigraphic unit. The source of the iron was either derived from pedogenic processes (top down) or hydrogeologic conditions within the subsurface. The iron must have been derived from overlying sediments if it were derived by soil-forming processes (MacFarlane, 1976; Singer, 1975; Bourman and Ollier, 2002). Typically, the formation of a ferricrete through pedogenic processes results in a distinctive soil profile that includes a mottled horizon and a bleached or pallid zone beneath the ferricrete layer (Tardy, 1992; Pickett, 2003). None of these pedogenically-derived, ferricrete-associated A or B soil horizons is present in the stratigraphic units that either overlie or underlie the Clayton Formation ferricrete layers. Additionally, the overlying unnamed clastic sediments are not consistent with the landscape reduction model of laterite (i.e., ferricrete) formation as proposed by McFarlane (1976). Therefore, the iron must have been derived from some other source.

FERRICRETES FROM GROUNDWATER

As previously noted, pedogenically-derived

Figure 2. Multiple ferricrete layers have developed at and near the base of the Clayton Formation (white layer beneath the lowest ferricrete layer is the Providence Formation). Oxidation of the former fluctuating potentiometric surface has created these ferricretes at varying levels within the shallow subsurface. Scale in 15-cm divisions.

Figure 3. Flat-lying, small-scale ferricrete layers have formed in the Clayton Formation at different elevations within the subsurface due to groundwater oxidation along a fluctuating potentiometric surface. Scale in centimeters and inches.

Figure 4. This groundwater-developed ferricrete is exposed near the contact between the Clayton Formation and the underlying Providence Formation. The iron-cemented layer likely reflects the oxidation contact in the zone of groundwater saturation within the subsurface. Scale in 15-cm divisions.

Figure 5. Multiple nested groundwater-developed ferricretes have formed oval-shaped concretions in the basal clayey sand of the Clayton Formation directly above the Providence Formation. Such ferricrete morphology reflects a complex zone of oxidation and is likely a result of lithologic variability.

Figure 6. This groundwater-developed ferricrete occurs at or near the base of the Clayton Formation and has formed around a diapir of clay derived from the underlying Providence Formation (see Marsalis and Friddell, 1975, p. 17). Scale in 15-cm divisions.

Figure 7. This groundwater-derived ferricrete within the Clayton Formation has developed along joints and fractures within the shallow subsurface. Scale in 15-cm divisions.

ferricretes would have been derived from overlying iron-containing geologic materials. However, this concept has been challenged, especially where the source of the iron minerals could not have been locally derived (Maignien, 1966; Ollier, 1991; Bourman, 1996). Recent studies on ferricretes have documented their development due to changes in groundwater pH/Eh geochemistry as a function of subsurface geology (Ferguson and others, 1983; Mann and Ollier, 1985; Bourman and others, 1987; Milnes and others, 1987; Wright and others, 1992; Bourman, 1993, 1996; Phillips and others, 1997; Furniss and others, 1999; Phillips, 1999; Chan and others, 2000; Phillips, 2000; De Hon and others, 2001; Yager and others, 2003; Froede and Rucker, 2006; Widdowson, 2007). The result of this work has been the identification of ferricretes in the shallow subsurface created not by soil-forming processes but by the oxidation of anaerobic and acidic ferrous groundwater.

FERRICRETE CLASSIFICATION AND MORPHOLOGY

Bourman and others (1987) divided ferricretes into three general categories: 1) ferruginized bedrock, 2) ferruginized sediments, and 3) complex ferricretes. In this classification scheme, the ferricrete layers in the marine clastic lithofacies of the Clayton Formation would be considered ferruginized sediment due to the authigenic iron mineral cements (i.e., ferrihydrite, goethite, limonite, and hematite) infilling the pore spaces in the clayey sand.

Groundwater-developed ferricretes can vary in their morphology. Traditionally, they have been viewed as subsurface features that mimic flat-lying ground surfaces (Maignien, 1966; McFarlane, 1976; Goudie, 1985). However, ferricretes can also develop in the subsurface parallel to sloped surfaces (Clare, 1960; Mulcahy, 1960; Phillips and others, 1997; Phillips, 1999, 2000) and along fractures and joints (Mann and Ollier, 1985).

FERRICRETES IN THE CLASTIC LITHOFACIES OF THE CLAYTON FORMATION

Ferricretes do not occur in all places in the Clayton Formation clastic sediments. However, where they do occur, they exhibit a wide range of shapes and sizes. Generally, the ferricretes can form as one or more intrastratal layers where conditions have allowed for the precipitation of the ferric minerals (Figures 2 and 3). They have also developed at or near the contact with the underlying Providence Formation (Figures 4 and 5). Some of the ferricretes have formed along joint and fracture surfaces within the subsurface resulting in the formation of complex shapes (Figures 6 and 7). Each of these ferricretes is a study unto itself and none have been studied in any detail. Further investigation of each of these varying forms is warranted and should yield details regarding their formation within the context of a variable groundwater table as a function of areal uplift and the oxidation of groundwater within the subsurface (see Tanner and Khalifa, 2010).

The Clayton Formation groundwater ferricretes have formed economic iron deposits at several locations across west-central Georgia. The ore was mined for many years (1950s to 1960s) in Stewart, Quitman, and Webster Counties (Furcron, 1956; Furcron and Ray, 1957; Reinhardt and others, 1994). Processing of the iron-rich ferricrete ore was conducted by ironworks in Birmingham, Alabama.

CONCLUSIONS

While originally interpreted as the product of limestone weathering, the ferricretes contained within the updip clastic lithofacies of the Clayton Formation are better defined as the product of hydrogeologic processes. Ferricrete development within these sediments occurred with the oxidation of anaerobic ferrous groundwater and the precipitation of ferrihydrite, goethite, limonite and hematite minerals. The ferricrete layers developed in the Clayton Formation clastic lithofacies and/or at or near the contact with the underlying Providence Formation. Their variable

morphology is a direct result of subsurface sedimentary and structural features and a dynamic water table. Further investigation of these subsurface features is warranted and should yield details regarding their formation within the context of a variable groundwater table, regional uplift, and the oxidation of anaerobic ferrous groundwater within the subsurface.

ACKNOWLEDGMENTS

I thank A.J. Akridge, J.K. Reed, and W.J. Neal for their constructive comments. Gratitude is expressed to M.D. Cocker for his time in the field examining outcrops of the Clayton Formation across west-central Georgia. Appreciation is conveyed to A. Giles and J. Costello for information related to ferricretes within the study area. Reference assistance was kindly provided by E.L. Williams, T. Harmon-Unongo, P. Vierheller, and K. Piselli. This work neither represents the views or opinions of the U.S. Environmental Protection Agency, nor was this investigation conducted in any official capacity. Any mistakes that may remain are my own.

REFERENCES CITED

Alhadeff, S.J., Musser, J.W., Sandercock, A.C., and Dyar, T.R., 2001, Digital environmental atlas of Georgia: Atlanta, GA, Georgia Geologic Survey CD-1.

Bourman, R.P., 1993, Modes of ferricrete genesis: Evidence from southeastern Australia: Zeitschrift für Geomorphologie, v. 37, p. 77-101.

Bourman, R.P., 1996, Towards distinguishing transported and in situ ferricretes: data from southern Australia: AGSO Journal of Australian Geology and Geophysics, v. 16, p. 231-241.

Bourman, R.P., Milnes, A.R., and Oades, J.M., 1987, Investigations of ferricretes and related surficial ferruginous materials in parts of southern and eastern Australia: Zeitschrift für Geomorphologie, v. 64, p. 1-24.

Bourman, R.P., and Ollier, C.D., 2002, A critique of the Schellman definition and classification of "laterite": Catena, v. 47, p. 117-131.

Chan, M.A., Parry, W.T., and Bowman, J.R., 2000, Diagenetic hematite and manganese oxides and fault-related fluid flow in Jurassic sandstones, southeastern Utah: American Association of Petroleum Geologists Bulletin, v. 84, p. 1281-1310.

Clare, K.E., 1960, Roadmaking gravels and soils in central Africa: Middlesex, UK, Overseas Bulletin 12, Road Research Laboratory.

Cocker, M.D., 2006, Geologic atlas of the Brooksville, Cuthbert, Georgetown, and Martins Crossroads, Georgia 7.5 minute quadrangles: Atlanta, GA, Georgia Geologic Survey, Open File Report 06-1.

Cooke, C.W., 1943, Geology of the coastal plain of Georgia: Washington, DC, U.S. Geological Survey Bulletin 941.

De Hon, R.A., Washington, P.A., Glawe, L.N., Young, L.M., and Morehead, E.A., 2001, Formation of northern Louisiana ironstones: Gulf Coast Association of Geological Societies Transactions, v. 51, p. 55-61.

Donovan, A.A., 1986, Sedimentology of the Providence Formation, *in* Reinhardt, J., ed., Stratigraphy and sedimentology of continental, nearshore, and marine Cretaceous sediments of the eastern Gulf Coastal Plain: Atlanta, GA, Field trip 3, Georgia Geological Society, p. 29-44.

Eargle, D.H., 1955, Stratigraphy of the outcropping Cretaceous rocks of Georgia: Washington, DC, U.S. Geological Survey Bulletin 1014.

Ferguson, J., Burne, R.V., and Chambers, L.A., 1983, Iron mineralization of peritidal carbonate sediments by continental groundwaters, Fisherman Bay, South Australia: Sedimentary Geology, v. 34, p. 41-57.

Froede, C.R., Jr., 2008, Defining the nearshore marine to fluvial transition in the updip clastic lithofacies of the Clayton Formation (Lower Paleocene) across the west-central Georgia coastal plain (USA): Southeastern Geology, v. 46, p. 25-35.

Froede, C.R., Jr., 2010. Sedimentary and stratigraphic evidence of a sea-level regression due to tectonism and eustatic decline: Geologic guidebook to Providence Canyon State Park and surrounding vicinity (Stewart County, Georgia): Atlanta, Georgia, American Institute of Professional Geologists field trip guidebook.

Froede, C.R., Jr., and Reed, J.K. 2007, Subaqueous karstification of the top of the Clayton Formation limestone (lower Paleocene) near Ft. Gaines, Georgia (USA): Southeastern Geology, v. 45, p. 87-96.

Froede, C.R., Jr., and Rucker, B.R., 2006, Iron Mountain, Santa Rosa County, Florida: A paleogroundwater table inverted relief feature: Southeastern Geology, v. 44, p. 137-145.

Furcron, A.S., 1956, Iron ores of the Clayton Formation in Stewart and Quitman Counties, Georgia: Georgia Mineral Newsletter, v. 9, p. 116-124.

Furcron, A.S., and Ray, D.L., 1957, Clayton iron ores of Webster County, Georgia: Georgia Mineral Newsletter, v. 10, p. 73-76.

Furniss, G., Hinman, N.W., Doyle, G.A., and Runnells, D.D., 1999, Radiocarbon-dated ferricrete provides a record of natural acid rock drainage and paleoclimatic changes: Environmental Geology, v. 37, p. 102-106.

Gibson, T.G., 1980, Facies changes of lower Paleogene strata: Upper Cretaceous and lower Tertiary geology of the Chattahoochee River Valley, western Georgia and eastern Alabama, *in* Frey, R.W., ed., Excursions in Southeastern Geology, Volume II: Falls Church, VA, American Geological Institute, field trip guidebook, p.

402-411.

Gibson, T.G., 1982, Paleocene to middle Eocene depositional cycles in eastern Alabama and western Georgia, *in* Arden, D.D., Beck, B.F., and Morrow, E., eds., Proceedings of the second symposium on the geology of the southeastern Coastal Plain: Atlanta, GA, Georgia Geologic Survey, Information Circular 53, pp. 53-63.

Gibson, T.G., 1992, Lithologic changes in fluvial to marine depositional systems in Paleogene strata of Georgia and Alabama, *in* Gohn, G.S., ed., Proceedings of the 1988 U.S. Geological Survey workshop on the geology and geohydrology of the Atlantic Coastal Plain: Washington, DC, U.S. Geological Survey, Circular 1059, p. 109-113.

Goudie, A.S., 1985, Duricrusts and landforms, *in* Richards, K.S., Arnett, R.R., and Ellis, S., eds., Geomorphology and soils: Boston, MA, Allen and Unwin, p. 37-57.

Maignien, R., 1966, Review of research on laterites: Paris, France, United Nations Educational, Scientific and Cultural Organization.

Mann, A.W., and Ollier, C.D., 1985, Chemical diffusion and ferricrete formation: Catena Supplement 6, Soils and Geomorphology, v. 6, p. 151-157.

Marsalis, W.E., and Friddell, M.S., 1975, A guide to selected Upper Cretaceous and lower Tertiary outcrops in the lower Chattahoochee River Valley of Georgia: Atlanta, Georgia, Georgia Geological Society field trip guidebook 15.

McFarlane, M.J., 1976, Laterite and landscape: New York, NY, Academic Press.

Milnes, A.R., Bourman, R.P., and Fitzpatrick, R.W., 1987, Petrology and mineralogy of "laterites" in southern and eastern Australia and southern Africa: Chemical Geology, v. 60, p. 237-250.

Mulcahy, M.J., 1960, Laterites and lateritic soils in southwestern Australia: Journal of Soil Science, v. 11, p. 206-225.

Ollier, C.D., 1991, Laterite profiles, ferricrete and landscape evolution: Zeitschrift für Geomorphologie, v. 35, p. 165-173.

Phillips, J.D., 1999, Edge effects in geomorphology: Physical Geography, v. 20, p. 53-66.

Phillips, J.D., 2000, Rapid development of ferricretes on a subtropical valley side slope: Geografiska Annaler, v. 82-A, p. 69-78.

Phillips, J.D., Lampe, M., King, R.T., Cedillo, M., Beachley, R., and Grantham, C., 1997, Ferricrete formation in the North Carolina Coastal Plain: Zeitschrift für Geomorphologie, v. 41, p. 67-79.

Pickett, J.W., 2003, Stratigraphic relationships of laterite at Little Bay, near Marouba, New South Wales: Australian Journal of Earth Sciences, v. 50, p. 63–68.

Reinhardt, J., and Gibson, T.G., 1981, Upper Cretaceous and lower Tertiary geology of the Chattahoochee River Valley, western Georgia and eastern Alabama, *in* Frey, R.W., ed., Excursions in southeastern geology, Volume II: Falls Church, VA, American Geological Institute, p. 385-463.

Reinhardt, J., Schindler, J.S., and Gibson, T.G., 1994, Geologic map of the Americus 30' X 60' quadrangle, Georgia and Alabama: Washington, DC, U.S. Geological Survey, Miscellaneous Investigations Series, Map I-2174.

Singer, A., 1975, A Cretaceous laterite in the Negev Desert, southern Israel: Geological Magazine, v. 112, p. 151-162.

Tanner, L.H., and Khalifa, M.A., 2010, Origin of ferricretes in fluvial-marine deposits of the lower Cenomanian Bahariya Formation, Bahariya Oasis, Western Desert, Egypt: Journal of African Earth Sciences, v. 56, p. 179-189.

Tardy, Y., 1992, Diversity and terminology of lateritic profiles, *in* Martini, I.P., and Chesworth, W., eds., Weathering, Soils and Paleosols: Amsterdam, Elsevier, pp. 379–405.

Veatch, O., and Stephenson, L.W., 1911, Preliminary report on the geology of the coastal plain of Georgia: Atlanta, GA, Geological Survey of Georgia Bulletin 26.

Widdowson, M., 2007, Laterite and ferricrete, *in* Nash, D.J., and McLaren, S.J., eds., Geochemical sediments and landscapes: Malden, Massachusetts, Blackwell, p. 46-94.

Wright, V.P., Sloan, R.J., Valero Garcés, B., Garvie, L.A.J., 1992, Groundwater ferricretes from the Silurian of Ireland and Permian of the Spanish Pyrenees: Sedimentary Geology, v. 77, p. 37-49.

Yager, D.B., Church, S.E., Verplanck, P.L., and Wirt, L., 2003, Ferricrete, manganocrete, and bog iron occurrences with selected sedge bogs and active iron bogs and springs in the upper Animas River Watershed, San Juan County, Colorado: Washington, DC, U.S. Geological Survey, Miscellaneous Field Studies Map MF-2406.